


RESEARCH

Open Access



# Exosomal long noncoding RNA MLETA1 promotes tumor progression and metastasis by regulating the miR-186-5p/EGFR and miR-497-5p/IGF1R axes in non-small cell lung cancer

Xiu-Rui Hsu<sup>1</sup>, Jia-En Wu<sup>1</sup>, Yi-Ying Wu<sup>2</sup>, Sheng-Yen Hsiao<sup>1,3</sup>, Jui-Lin Liang<sup>1,4</sup>, Ya-Ju Wu<sup>5</sup>, Chia-Hao Tung<sup>1</sup>, Meng-Fan Huang<sup>1</sup>, Ming-Shiu Lin<sup>6</sup>, Pan-Chyr Yang<sup>6,7,8</sup>, Yuh-Ling Chen<sup>9\*</sup>  and Tse-Ming Hong<sup>1,2\*</sup>

## Abstract

**Background** Lung cancer is the most common and deadliest cancer worldwide, and approximately 90% of all lung cancer deaths are caused by tumor metastasis. Tumor-derived exosomes could potentially promote tumor metastasis through the delivery of metastasis-related molecules. However, the function and underlying mechanism of exosomal long noncoding RNA (lncRNA) in lung cancer metastasis remain largely unclear.

**Methods** Cell exosomes were purified from conditioned media by differential ultracentrifugation and observed using transmission electron microscopy, and the size distributions were determined by nanoparticle tracking analysis. Exosomal lncRNA sequencing (lncRNA-seq) was used to identify long noncoding RNAs. Cell migration and invasion were determined by wound-healing assays, two-chamber transwell invasion assays and cell mobility tracking. Mice orthotopically and subcutaneously xenografted with human cancer cells were used to evaluate tumor metastasis in vivo. Western blot, qRT-PCR, RNA-seq, and dual-luciferase reporter assays were performed to investigate the potential mechanism. The level of exosomal lncRNA in plasma was examined by qRT-PCR. MS2-tagged RNA affinity purification (MS2-TRAP) assays were performed to verify lncRNA-bound miRNAs.

**Results** Exosomes derived from highly metastatic lung cancer cells promoted the migration and invasion of lung cancer cells with low metastatic potential. Using lncRNA-seq, we found that a novel lncRNA, lnc-MLETA1, was upregulated in highly metastatic cells and their secreted exosomes. Overexpression of lnc-MLETA1 augmented cell migration and invasion of lung cancer. Conversely, knockdown of lnc-MLETA1 attenuated the motility and metastasis of lung cancer cells. Interestingly, exosome-transmitted lnc-MLETA1 promoted cell motility and metastasis of lung cancer. Reciprocally, targeting lnc-MLETA1 with an LNA suppressed exosome-induced lung cancer cell motility. Mechanistically, lnc-MLETA1 regulated the expression of EGFR and IGF1R by sponging miR-186-5p and miR-497-5p to facilitate cell motility. The clinical datasets revealed that lnc-MLETA1 is upregulated in tumor tissues and predicts

\*Correspondence:

Yuh-Ling Chen

yuhling@ncku.edu.tw

Tse-Ming Hong

tmhong@ncku.edu.tw

Full list of author information is available at the end of the article



© The Author(s) 2023. **Open Access** This article is licensed under a Creative Commons Attribution 4.0 International License, which permits use, sharing, adaptation, distribution and reproduction in any medium or format, as long as you give appropriate credit to the original author(s) and the source, provide a link to the Creative Commons licence, and indicate if changes were made. The images or other third party material in this article are included in the article's Creative Commons licence, unless indicated otherwise in a credit line to the material. If material is not included in the article's Creative Commons licence and your intended use is not permitted by statutory regulation or exceeds the permitted use, you will need to obtain permission directly from the copyright holder. To view a copy of this licence, visit <http://creativecommons.org/licenses/by/4.0/>. The Creative Commons Public Domain Dedication waiver (<http://creativecommons.org/publicdomain/zero/1.0/>) applies to the data made available in this article, unless otherwise stated in a credit line to the data.

survival in lung cancer patients. Importantly, the levels of exosomal lnc-MLETA1 in plasma were positively correlated with metastasis in lung cancer patients.

**Conclusions** This study identifies lnc-MLETA1 as a critical exosomal lncRNA that mediates crosstalk in lung cancer cells to promote cancer metastasis and may serve as a prognostic biomarker and potential therapeutic target for lung cancer diagnosis and treatment.

**Keywords** lnc-MLETA1, Lung cancer metastasis, Exosome, miR-186-5p, miR-497-5p, IGF1R, EGFR

## Background

Lung cancer is the most common and deadliest cancer worldwide [1]. Non-small cell lung cancer (NSCLC) accounts for approximately 85% of all lung cancers [2]. NSCLC patients have no typical clinical symptoms in the early stages; thus, most patients are diagnosed with advanced-stage disease at the time of their initial diagnosis, and the five-year survival rate is less than 10% [3, 4]. In addition, approximately 90% of all lung cancer-related deaths are due to metastasis. Therefore, elucidation of the underlying mechanisms of lung cancer metastasis and identification of early biomarkers for lung cancer diagnostics and treatment are urgently needed.

Exosomes are extracellular membrane nanovesicles (30–150 nm) that can be secreted by most types of cells, including immune cells, fibroblasts, adipocytes, epithelial cells, and especially tumor cells [5]. Emerging evidence indicates that exosomes can potentially facilitate cell motility and tumor metastasis through the transfer of protein and noncoding RNA [6]. For instance, Shang et al. found that exosome-delivered circPACRGL promotes colorectal cancer cell migration and invasion through the miR-142-3p/miR-506-3p-TGF- $\beta$ 1 axis [7]. Wang et al. found that exosome-derived GIPC2 facilitates prostate cancer metastasis via the activation of WNT- $\beta$ -catenin cascades [8]. Qiu et al. found that exosome-transmitted miR-519a-3p enhances liver metastasis by targeting DUSP2 and activating the MAPK/ERK pathway [9]. These studies suggest that exosomes play an important role in intercellular communication and are involved in tumor progression and metastasis.

Long noncoding RNAs (lncRNAs) are a class of transcripts that are longer than 200 nucleotides and lack protein-coding ability [10]. Accumulating evidence has shown that lncRNAs are involved in multiple regulatory mechanisms of gene expression and modulate many physiological and pathological functions, such as metabolism, proliferation, apoptosis, drug resistance, and especially tumor metastasis [11–16]. Recent studies have suggested that the molecular mechanisms of lncRNAs depend on lncRNA cellular localization [17]. In the cytoplasm, lncRNAs participate in post-transcriptional modification by acting as competing endogenous RNAs to decoy microRNAs and increase the expression of

downstream targets. Moreover, lncRNAs can enhance protein stability by directly interacting with the target protein and influence mRNA translation by complementarily binding to mRNAs. In the nucleus, lncRNAs can be involved in transcriptional regulation by recruiting transcription factors or modifying transcription factor activity. Recently, many studies have revealed that lncRNAs modulate tumor metastasis in various cancers [18]. For example, Li et al. found that lncRNA UBE2CP3 promotes gastric cancer metastasis by regulating the miR-138-5p/ITGA2 axis [19]. Wu et al. found that LINC00941 facilitates colorectal cancer metastasis by directly binding the SMAD4 protein and competing with ubiquitin ligase to prevent SMAD4 protein degradation [20]. Wen et al. found that lncRNA NEAT1 promotes lung and bone metastasis of prostate cancer by modulating Pol II ser2 phosphorylation [21]. Collectively, these studies suggest that lncRNAs play a critical role in tumor metastasis. In addition, some studies have shown that exosomal lncRNAs participate in lung cancer aggressiveness and anti-cancer therapy resistance [22–25]. However, the effect and mechanism of exosomal lncRNAs on lung cancer metastasis is still unknown.

In this study, we found a novel lncRNA, ENST00000563763, that was upregulated in highly metastatic lung cancer cells and their secreted exosomes. Therefore, we named this lncRNA metastatic lung cancer cell-derived exosome transmitted lncRNA 1 (MLETA1). Functional assays indicated that lnc-MLETA1 promoted cell motility and metastasis in lung cancer. Interestingly, exosome-transmitted lnc-MLETA1 facilitated cell motility and metastasis of lung cancer. Mechanistically, lnc-MLETA1 regulated the expression of EGFR and IGF1R and promoted cell motility by sponging miR-186-5p and miR-497-5p. Our findings suggest that lnc-MLETA1 plays a key role in lung cancer metastasis and may serve as a novel biomarker and potential therapeutic target for lung cancer diagnostics and treatment.

## Methods

### Cell culture

The human lung adenocarcinoma cell line CL1-0 and CL1-5 cells were cultured in RPMI 1640 medium supplemented with 10% fetal bovine serum (FBS, Gibco). The

stable cells were selected in RPMI 1640 medium supplemented with 10% FBS and 800  $\mu\text{g}/\text{ml}$  G418. All cells were cultured in a humidified atmosphere containing 5%  $\text{CO}_2$  at 37 °C.

#### Conditioned media harvest

CL1-0 ( $1 \times 10^6$  cells) and CL1-5 ( $1 \times 10^6$  cells) were seeded in 100-mm dishes. After 24 h, the cells were washed with phosphate buffered saline (PBS) two times and were incubated in RPMI-1640 medium containing exosome-depleted FBS for 48 h. After incubation, the conditioned media were harvested and centrifuged at 300 g for 15 min and at 2,000 g for 15 min at 4 °C to remove cells.

#### Purification of exosomes by differential ultracentrifugation

CL1-0 ( $1 \times 10^6$  cells) and CL1-5 ( $1 \times 10^6$  cells) were seeded in 100-mm dishes. After 24 h, the cells were washed with PBS two times and incubated in RPMI-1640 medium containing exosome-depleted FBS for 48 h. After incubation, exosomes were purified from the conditioned media by differential ultracentrifugation. Briefly, conditioned media were centrifuged at 300 g for 15 min and at 2,000 g for 15 min at 4 °C to remove cells. And then supernatant was centrifuged at 10,000 g for 45 min at 4 °C to remove cell debris. Finally, exosomes were pelleted by ultracentrifugation at 100,000 g for 70 min at 4 °C. Exosomes were resuspended in PBS and collected by ultracentrifugation again at 100,000 g for 70 min.

#### Transmission electron microscopy

10  $\mu\text{l}$  of exosomes were dropped onto Formvar-carbon-coated 200-mesh copper electron microscopy grids, incubated for 5 min at room temperature (RT) and the excess solution were removed by filter paper. After stained by 2% uranyl acetate for 1 min at RT, the grids were washed with  $\text{ddH}_2\text{O}$  twice. The samples were observed using transmission electron microscopy.

#### Nanoparticle tracking analysis

Analysis of absolute size distribution and concentration of exosomes were determined using Nanoparticle tracking analysis. Exosomes were diluted in 1 ml PBS and mixed well, then the diluted exosomes were injected into the NanoSight NS300 instrument, and particles were automatically tracked and sized based on Brownian motion and the diffusion coefficient. Filtered PBS was used as controls.

#### Western blot analysis

Cells were washed with PBS two times and lysed in RIPA lysis buffer containing 0.25% Sodium deoxycholate, 0.1% SDS a, 1% Triton X-100 in  $1 \times \text{PBS}$ , 1 mM  $\text{Na}_3\text{VO}_4$ , 10 mM NaF, and protease inhibitor (Roche), for

10 min on ice. After collecting the cell lysates by scraping, centrifuged the lysates at 12,000 rpm for 30 min at 4 °C. Collected clear supernatants and measured protein concentration using a Bradford protein assay (Bio-Rad). The cell lysates (20  $\mu\text{g}$ ) and exosomes (10  $\mu\text{l}$ ) were loaded and proteins were separated by 10% sodium dodecyl sulfate polyacrylamide gel electrophoresis (SDS-PAGE). Next, the protein was transferred to PVDF membrane (0.45  $\mu\text{m}$ , Millipore) in transfer buffer at 400 mA for 1 h and blocked in 0.1% TBST with 5% non-fat milk for 1 h. Subsequently, the membrane was probed with primary antibodies in 0.1% TBST with 5% BSA at 4 °C overnight. Then blots were incubated with the appropriate horseradish peroxidase-conjugated (HRP-conjugated) secondary antibodies (Jackson ImmunoResearch) in 0.1% TBST with 5% non-fat milk at RT for 1 h, and the bound antibodies were visualized using ECL staining (PerkinElmer).

#### Antibodies

Primary antibodies used for immunoblotting were listed below: anti-CD9 (D8O1A; Cell Signaling), anti-TSG101 (GTX118736; GeneTex), anti-Flotillin-1 (GTX104769; GeneTex), anti-Calnexin (GTX109669; GeneTex), anti-GFP (sc-9996; Santa Cruz), anti-Ago2 (ab186733; Abcam), anti-GST (M0006; AbOmics), anti-EGFR (#2232; Cell Signaling), anti-IGF1R (D23H3; Cell Signaling), anti- $\beta$ -Actin (AC-15; Sigma-Aldrich).

#### In vitro wound-healing assay

In vitro wound-healing assays were performed with Ibidi Culture-Inserts (Blossom Biotechnologies). CL1-0 ( $1.8 \times 10^4$  cells) and CL1-5 ( $3 \times 10^4$  cells) were seeded in each insert for 24 h, and the inserts were removed. Photographs were taken at 0, 10, 16 and 24 h in the wound gap with 40 $\times$  magnification. Finally, the number of migrated cells was counted.

#### Transwell invasion assay

Transwell invasion assays were performed with 24-well polycarbonate Transwell filters (pore size 8  $\mu\text{m}$ , Costar 3422) coated with 30  $\mu\text{g}$  of Matrigel (BD Biosciences, NY, USA). CL1-0 ( $1.8 \times 10^4$  cells) and CL1-5 ( $3 \times 10^4$  cells) were seeded in the upper chamber containing serum-free medium, and RPMI-1640 medium containing 10% FBS were added in the lower chamber for 24 h and 16 h, respectively. On the upper surface of the filter, non-penetrating cells were removed with a cotton swab. Penetrating cells were stained by Liu's stain (ASK). Finally, the number of invaded cells was counted at 40 $\times$  magnification in five different fields per filter.

### RNA-sequencing analysis

Total RNA was fragmented through heat treatment and then reverse transcribed into cDNA using random primers and reverse transcriptase. Library construction was completed by performing end trimming, adding adapters, PCR amplification, and magnetic bead purification. Quality-verified libraries were sequenced on the Illumina NovaSeq 6000 platform with a specification of 150 PE sequencing. The raw data was processed using fastp to eliminate low-quality bases, adapters, and reads containing excessive unknown bases (N), resulting in clean reads. After removing ribosomal RNA, the reads depleted of rRNA were aligned to the reference genome. Differential gene expression analysis was conducted and identified using edgeR.

### Cell proliferation assay

lnc-MLETA1-knockdown and control CL1-5 cells ( $3 \times 10^3$  cells per well) were seeded in 100  $\mu$ l medium in a 96-well plate. Proliferation was measured every 24 h. After removing the culture medium, 90  $\mu$ l medium mixed with 10  $\mu$ l WST-1 reagent (Roche) were added to each well. After 40 min incubation, cell viability was determined by measuring the absorbance at 450 nm using a microplate reader.

### Soft-agar colony formation assay

lnc-MLETA1-knockdown or control CL1-5 cells ( $3 \times 10^3$  cells per well) in RPMI medium containing 0.35% agarose gel were seeded into 6-well plates containing 0.7% agarose gel in the lower layer. The plates were incubated at 37 °C with 5% CO<sub>2</sub> for 2 weeks to facilitate foci formation. Subsequently, the colonies were stained with 0.1% crystal violet and counted under a microscope.

### Cellular RNA isolation

The cells in 60-mm dish were lysed with 1 ml TRIzol reagent (Invitrogen) at RT for 10 min. Then the lysate was added 200  $\mu$ l of chloroform. The mixture was incubated at RT for 3 min and then centrifuged at 12,000 rpm for 20 min at 4 °C. The upper supernatant was transferred into fresh tube and added 500  $\mu$ l isopropanol. The mixture was incubated at RT for 10 min and then centrifuged at 12,000 rpm for 20 min at 4 °C. Then upper supernatant was completely removed. The RNA pellet was washed in 1 ml cold 75% ethanol in DEPC-ddH<sub>2</sub>O and centrifuged at 12,000 rpm for 10 min at 4 °C. Finally, the RNA pellet was air-dried for 10 min and then dissolved in 20  $\mu$ l DEPC-ddH<sub>2</sub>O.

### Exosomal RNA isolation

Total RNA from exosomes were extracted by the Direct-zol™ RNA kit (Zymo Research) following the manufacturer's instructions.

### Quantitative real-time polymerase chain reaction (qRT-PCR)

The purity and concentration of isolated RNA were determined by Nanodrop. 1  $\mu$ g of cellular total RNA or 20 ng of exosomal total RNA were reverse-transcribed to cDNA using the Random Hexamers by SuperScript III Reverse Transcriptase (Invitrogen). Quantitative RT-PCR analysis were performed using the SYBR Green PCR Master Mix (Applied Biosystems). GAPDH, 18S rRNA and U6 snRNA were used for normalization.

### Plasmid construction

The cDNA of lncRNA was amplified by AccuPrime Pfx DNA Polymerase (Invitrogen) and subcloned into the pcDNA3.1 (+) vector.

### Transfection

CL1-0 ( $4 \times 10^5$  cells) and CL1-5 ( $4 \times 10^5$  cells) were seeded in 60-mm dishes. After 24 h, plasmids and locked nucleic acid (LNA™) were transfected into the cells using Lipofectamine™ 2000 transfection reagents (Invitrogen) and Lipofectamine™ RNAiMAX transfection reagent (Invitrogen), respectively. 12.5  $\mu$ l lipofectamine 2000 or 18  $\mu$ l lipofectamine RNAiMAX was mixed with 600  $\mu$ l OPTI-MEM medium (Gibco) and 5  $\mu$ g plasmids or 6  $\mu$ l locked nucleic acid was mixed with another 600  $\mu$ l OPTI-MEM medium. After incubation at RT for 5 min, the two mixtures were mixed together. After incubation at RT for 20 min, the culture medium was removed, and the cells were washed with PBS. Then the mixture was added into cells and cells were incubated at 37 in 5% CO<sub>2</sub>. After 4–6 h, the culture medium was replaced with fresh medium. Post 48-h post-transfection, functional assay was performed on the cells.

### MS2-tagged RNA affinity purification

MS2-tagged RNA affinity purification was performed as previously described [26]. Briefly, CL1-0 cells were co-transfected with either 6  $\mu$ g of pMS2-lnc-MLETA1 or pMS2 along with 2  $\mu$ g of pMS2-GST. Following 48 h of transfection, the cells were lysed in 1000  $\mu$ l of lysis buffer containing 20 mM Tris-HCl at pH 7.5, 100 mM KCl, 5 mM MgCl<sub>2</sub>, 0.5% NP-40, 10 mM dithiothreitol (DTT), protease inhibitors, and RNase inhibitor. The supernatant was incubated with a slurry of 50  $\mu$ l glutathione (GSH) agarose beads overnight at 4 °C, followed by washing with NT2 buffer containing 50 mM Tris-HCl at pH 7.5,

150 mM NaCl, 1 mM MgCl<sub>2</sub>, and 0.05% NP-40. Western blot analysis was performed using primary antibodies against Ago2 and glutathione S-transferase (GST). For the qRT-PCR assay, the supernatant was incubated with 0.1% SDS and 0.5 mg/ml Proteinase K for RNA purification before validating the expression levels of lncRNAs and miRNAs.

#### Xenograft animal model

For orthotopic xenograft model,  $1 \times 10^5$  CL1-5-GL or lnc-MLETA1-knockdown cells were suspended in 10  $\mu$ l PBS and mixed with 10  $\mu$ l Matrigel and intrapulmonary injection transplanted into the right lung of 6~8-week-old male nonobese diabetic/severe combined immunodeficiency (NOD-SCID) mice. After inoculation, tumor cells metastasizing from the right lung to the left lung were monitored and evaluated by the IVIS spectrum in vivo imaging system (PerkinElmer) every week for 4 weeks. After the mice were sacrificed, the whole lung was excised, formalin-fixed, paraffin-embedded, and subjected to hematoxylin–eosin staining. The number and size of tumor metastasis in the lung were observed and counted under a microscope. For subcutaneous xenograft model,  $1 \times 10^6$  CL1-0-GL cells were suspended in 100  $\mu$ l PBS and mixed with 100  $\mu$ l Matrigel and subcutaneously injection transplanted into the NOD-SCID mice. After inoculation, NOD-SCID mice were injected intratumorally with 20  $\mu$ g exosomes derived from lnc-MLETA1-overexpressing or control CL1-0 cells twice a week and the lung metastasis were monitored and evaluated by IVIS spectrum in vivo imaging system for 6 weeks. After the mice were sacrificed, the whole lung was excised, formalin-fixed, paraffin-embedded, and subjected to hematoxylin–eosin staining. The number and size of tumor metastasis in the lung were observed and counted under a microscope. The animal study protocol was approved by the Institutional Animal Care and Use Committee of

National Cheng Kung University (IACUC Approval No. 107119, Tainan, Taiwan).

#### Statistical analysis

All statistical analyses were performed using GraphPad Prism 8.0. Results are presented as mean  $\pm$  SD. A *P*-value < 0.05 was considered significant. The survival rate data of lung cancer patients were downloaded from the KM Plotter Online Tool (<http://www.kmplot.com>) and were analyzed by Kaplan–Meier analysis with the log-rank test. The correlation of exosomal lnc-MLETA1 levels isolated from plasma samples of lung cancer patients with clinical characteristics was analyzed using the Chi-squared test.

#### Results

##### Exosomes derived from highly metastatic lung cancer cells promote cell migration and invasion of poorly metastatic lung cancer cells.

To determine whether exosomes derived from highly metastatic CL1-5 lung cancer cells could enhance the migratory and invasive abilities of poorly metastatic CL1-0 lung cancer cells, we incubated CL1-0 cells with conditioned media from CL1-0 and CL1-5 cells. Wound-healing assays and transwell invasion assays showed that conditioned media from CL1-5 cells significantly increased the migration and invasion of CL1-0 cells compared with CL1-0 conditioned media (Fig. 1A and B). To further determine whether the effect of conditioned media on cell motility is mediated by exosomes, we performed a wound-healing assay on CL1-0 cells incubated with exosome-depleted conditioned media from CL1-0 and CL1-5 cells. The results showed that the exosome-depleted conditioned medium of CL1-5 cells had no significant influence on CL1-0 cell migration (Fig. 1C). These data suggested that the increased migratory and invasive abilities of CL1-0 cells are primarily due to the

(See figure on next page.)

**Fig. 1** Exosomes derived from high metastatic lung cancer cells promotes cell migration and invasion of low metastatic lung cancer cells. **A** Upper: representative images of wound-healing assay of CL1-0 cells pre-incubated with CL1-0 or CL1-5 conditioned media for 48 h. Scale bar, 200  $\mu$ m. Lower: the number of migrated cells was calculated. **B** Upper: representative images of transwell invasion assay of CL1-0 cells pre-incubated with CL1-0 or CL1-5 conditioned media for 48 h. Scale bar, 200  $\mu$ m. Lower: the number of invaded cells was calculated. **C** Upper: representative images of wound-healing assay of CL1-0 cells pre-incubated with CL1-0 or CL1-5 exosome-depleted conditioned media for 48 h. Scale bar, 200  $\mu$ m. Lower: the number of migrated cells was calculated. **D** Representative transmission electron microscopy images of exosomes derived from CL1-0 and CL1-5 cells. Scale bar, 200 nm. **E** Nanoparticle tracking analysis of the size distributions and number of exosomes derived from CL1-0 and CL1-5 cells. **F** Western blot analysis of exosome marker CD9, TSG101 and Flotillin-1 in CL1-0 and CL1-5 cells and exosomes. Calnexin was used as the negative controls. **G** Immunofluorescence assay of GFP in CL1-0 cells pre-incubated with CD9-GFP containing exosomes derived from CL1-0 or CL1-5 cells. Cells were stained with rhodamine phalloidin and DAPI for F-actin and nuclei, respectively. White arrowheads indicate the CD9-GFP containing exosomes. Scale bar, 20  $\mu$ m. **H** Left: representative images of wound-healing assay of CL1-0 cells pre-incubated with CL1-0 or CL1-5 exosomes for 48 h. Scale bar, 200  $\mu$ m. Right: the number of migrated cells was counted. **I** Left: representative images of transwell invasion assay of CL1-0 cells pre-incubated with CL1-0 or CL1-5 exosomes for 48 h. Scale bar, 200  $\mu$ m. Right: the number of invaded cells was counted. Results are presented as mean  $\pm$  SD from three independent experiments. \**P* < 0.05. Two-tailed Student's *t*-test

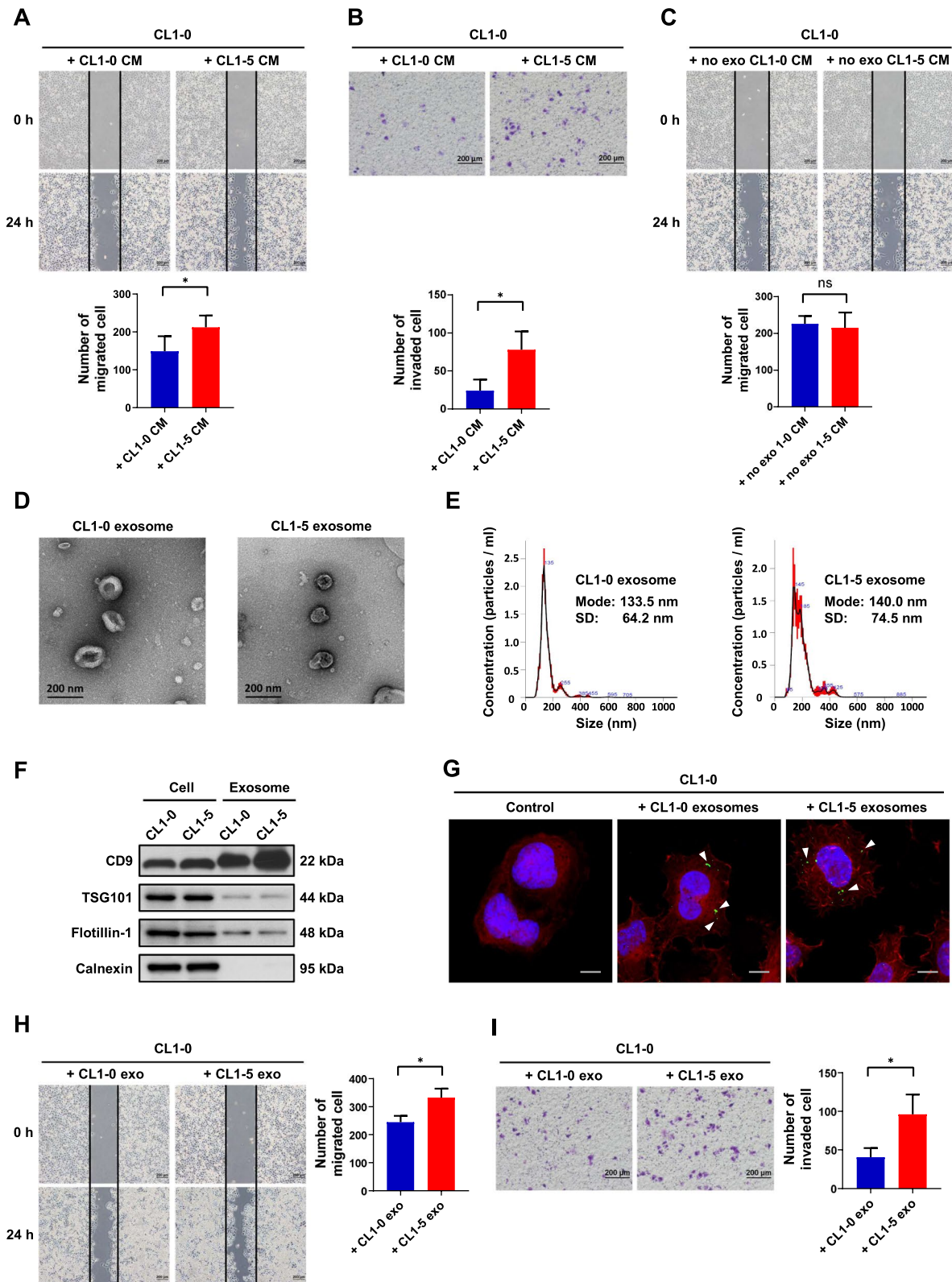


**Fig. 1** (See legend on previous page.)

transfer of exosomes from CL1-5 cells in the extracellular microenvironment.

To investigate the effect of exosomes derived from CL1-5 cells on the migratory and invasive abilities of CL1-0 cells, we isolated exosomes from the conditioned media of CL1-0 and CL1-5 cells by ultracentrifugation. The exosomes were characterized by transmission electron microscopy, western blot analysis and nanoparticle tracking analysis. Transmission electron microscopy of negatively stained exosomes revealed cup-shaped membrane vesicles (Fig. 1D). The nanoparticle tracking analysis indicated that the sizes of the exosomes derived from CL1-0 and CL1-5 cells were  $133.5 \pm 64.2$  nm and  $140.0 \pm 74.5$  nm, respectively (Fig. 1E). Western blot analysis showed the presence of the exosomal markers CD9, TSG101, and Flotillin-1 but not the endoplasmic reticulum protein calnexin in the exosomal samples (Fig. 1F). These data demonstrated that the vesicles purified from CL1-0 and CL1-5 cells were exosomes. To further determine whether exosomes can be directly transferred between cells, we isolated exosomes from the conditioned media of cells transiently transfected with the pEGFP-N-CD9 plasmid. Western blot analysis revealed that GFP was expressed in exosomes from the GFP-tagged CD9-overexpressing CL1-0 and CL1-5 cells (Supplementary Fig. S1A). Next, we incubated CL1-0 cells with CD9-GFP-containing exosomes for 8 h and observed GFP expression in the treated CL1-0 cells by confocal microscopy. The results showed that green fluorescence signals were detected in the treated CL1-0 cells but not in the untreated CL1-0 cells (Fig. 1G). These data indicated that exosomes derived from CL1-0 and CL1-5 cells can be taken up by CL1-0 cells. To determine whether exosome transfer from CL1-5 cells to CL1-0 cells can promote cell migration and invasion, we incubated CL1-0 cells with exosomes derived from CL1-0 and CL1-5 cells. Wound-healing assays and transwell invasion assays showed that exosomes derived from CL1-5 significantly increased the migration and invasion of CL1-0 cells compared with CL1-0 exosomes (Fig. 1H and I). Taken together, these

data suggested that the exosomes derived from CL1-5 cells facilitate cell migration and invasion of CL1-0 cells.

### lnc-MLETA1 promotes the migration and invasion of lung cancer cells in vitro

Recently, many studies have shown that exosomal miRNAs and proteins promote tumor metastasis [27–30]. However, the effect of exosomal lncRNAs on cell motility and tumor metastasis is still unknown. Therefore, we sought to explore whether exosomal lncRNAs can alter the motility of lung cancer cells. To identify lncRNAs in exosomes that may play roles in cell motility, we performed lncRNA sequencing on CL1-0 and CL1-5 exosomes. The heatmap showed the top 100 most increased and the top 50 most decreased lncRNAs among 489 differentially-expressed lncRNAs (fold change >5). There are 309 upregulated lncRNAs and 180 downregulated lncRNAs in CL1-5 exosomes compared with CL1-0 exosomes (Fig. 2A). The results showed that a novel lncRNA, ENST00000563763, was upregulated in CL1-5 exosomes compared with CL1-0 exosomes. We named it lnc-MLETA1 (metastatic lung cancer cell-derived exosome transmitted lncRNA 1). Next, we used qRT-PCR analysis to confirm the expression of several lncRNAs in CL1-0 and CL1-5 cells and their exosomes. The results showed that the expression of lnc-MLETA1 was highest in CL1-5 cells and exosomes compared with that of CL1-0 cells and exosomes (Fig. 2B and C). Moreover, we compared the expression of lnc-MLETA1 in poorly and highly metastatic lung cancer cells by qRT-PCR analysis and found that the expression of lnc-MLETA1 was significantly upregulated in highly metastatic lung cancer cells (Fig. 2D), suggesting that lnc-MLETA1 may be associated with the migratory and invasive abilities. Furthermore, the bioinformatic analysis showed that the sequence of lnc-MLETA1 was identified without protein-coding potential by Coding Potential Assessment Tool (CPAT) (Supplementary Fig. S1B). The secondary structure of lnc-MLETA1 was predicted by RNAfold web server (Supplementary Fig. S1C). lnc-MLETA1 is located on

(See figure on next page.)

**Fig. 2** lnc-MLETA1 promotes migration and invasion of lung cancer cells in vitro. **A** RNA-sequencing of total RNA extracted from CL1-0 exosomes and CL1-5 exosomes are presented in a heatmap. **B** and **C** qRT-PCR analysis of lnc-MLETA1 and other candidate lncRNA expression in CL1-0 and CL1-5 exosomes (**B**) and cells (**C**). **D** qRT-PCR analysis of lnc-MLETA1 expression between low metastatic cells and high metastatic lung cancer cells. **E** Left: representative images of wound-healing assay of lnc-MLETA1-overexpressing and control CL1-0 cells for 16 h. Scale bar, 200  $\mu$ m. Right: the number of migrated cells was counted. **F** Left: representative images of transwell invasion assay of lnc-MLETA1-overexpressing and control CL1-0 cells for 24 h. Scale bar, 200  $\mu$ m. Right: the number of invaded cells was counted. **G** Left: representative images of wound-healing assay of lnc-MLETA1-knockdown and control CL1-5 cells for 10 h. Scale bar, 200  $\mu$ m. Right: the number of migrated cells was counted. **H** Left: representative images of transwell invasion assay of lnc-MLETA1-knockdown and control CL1-5 cells for 16 h. Scale bar, 200  $\mu$ m. Right: the number of invaded cells was counted. **I** The XY position plots of single-cell tracking analysis of lnc-MLETA1-knockdown and control CL1-5 cells. **J** The path length and line length of cell migration of lnc-MLETA1-knockdown and control CL1-5 cells. Results are presented as mean  $\pm$  SD from three independent experiments. \* $P < 0.05$ , \*\* $P < 0.01$ , \*\*\* $P < 0.001$ . Two-tailed Student's *t*-test





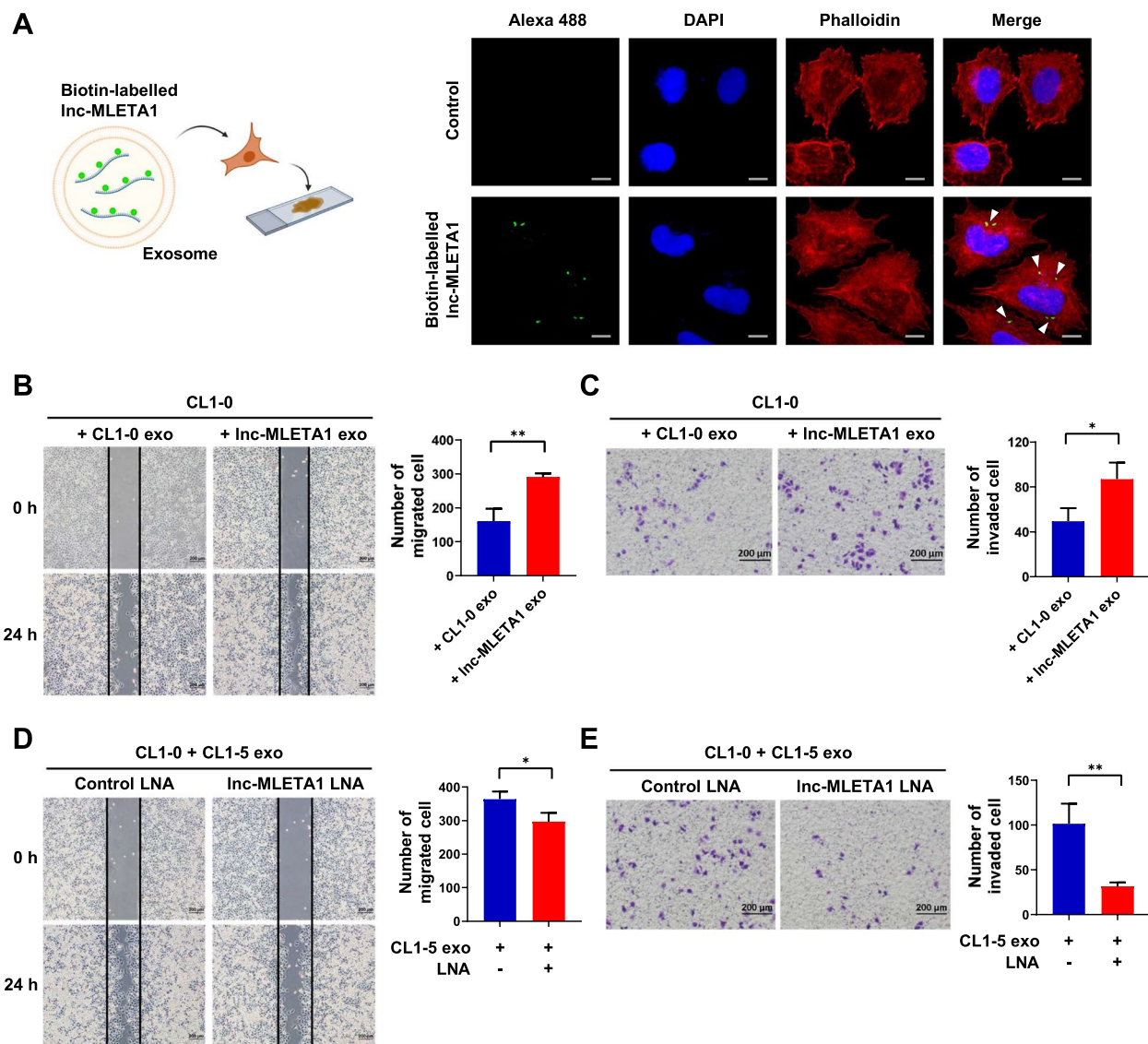


**Fig. 3** Exosomal Inc-MLETA1 promotes lung cancer cell migration and invasion in vitro. **A** Immunofluorescence assay of biotin-labelled Inc-MLETA1 in CL1-0 cells pre-incubated with exosomes derived from biotin-labelled Inc-MLETA1-transfected cells or control CL1-0 cells. Cells were stained with rhodamine phalloidin and DAPI for F-actin and nuclei, respectively. White arrowheads indicate the biotin-labelled Inc-MLETA1. Scale bar, 20  $\mu$ m. **B** Left: representative images of wound-healing assay of CL1-0 cells pre-incubated with exosomes derived from Inc-MLETA1-overexpressing or control CL1-0 cells for 48 h. Scale bar, 200  $\mu$ m. Right: the number of migrated cells was counted. **C** Left: representative images of transwell invasion assay of CL1-0 cells pre-incubated with exosomes derived from Inc-MLETA1-overexpressing or control CL1-0 cells for 48 h. Scale bar, 200  $\mu$ m. Right: the number of invaded cells was counted. **D** Left: representative images of wound-healing assay of CL1-0 cells pre-incubated with CL1-5 exosomes and transfected with Inc-MLETA1 LNA or control LNA for 48 h. Scale bar, 200  $\mu$ m. Right: the number of migrated cells was counted. **E** Left: representative images of transwell invasion assay of CL1-0 cells pre-incubated with CL1-5 exosomes and transfected with Inc-MLETA1 LNA or control LNA for 48 h. Scale bar, 200  $\mu$ m. Right: the number of invaded cells was counted. Results are presented as mean  $\pm$  SD from three independent experiments. \* $P < 0.05$ , \*\* $P < 0.01$ . Two-tailed Student's *t*-test

chromosome 17, near WSCD1 (Supplementary Fig. S1D). The ChIP-seq dataset GSE225332 indicated the enrichment of active histone markers, specifically H3K27ac and H3K4me3, within the genomic regions encompassing

Inc-MLETA1 in lung cancer cells, suggesting a more open and accessible chromatin structure (Supplementary Fig. S1E). In addition, we utilized the KM Plotter Online Tool to analyze the correlation between the expression

of lnc-MLETA1 and the survival rates of cancer patients, including AML, breast cancer, colon cancer, gastric cancer, myeloma, and ovarian cancer. The results showed that the expression of lnc-MLETA1 was not significantly correlated with patients' survival in AML, breast cancer, colon cancer, gastric cancer, myeloma, and ovarian cancer (Supplementary Fig. S1F-K). It seems that lnc-MLETA1 is specific and important for lung cancer.

To further determine the role of lnc-MLETA1 in cell motility, we overexpressed lnc-MLETA1 in CL1-0 cells by transfection of lnc-MLETA1 plasmids (Supplementary Fig. S2A). Wound-healing assays and transwell invasion assays showed that overexpression of lnc-MLETA1 significantly increased the migration and invasion of CL1-0 cells compared with those of the control group (Fig. 2E and F). Conversely, we silenced lnc-MLETA1 in CL1-5 cells by lentivirus-based short hairpin RNAs (shRNAs) (Supplementary Fig. S2B). Wound-healing assays and transwell invasion assays showed that the knockdown of lnc-MLETA1 significantly decreased the migration and invasion of CL1-5 cells compared with the controls (Fig. 2G and H). Moreover, single-cell tracking analysis revealed that knockdown of lnc-MLETA1 significantly decreased the path length and line length of CL1-5 cell migration compared with those in the control group (Fig. 2I and J). Furthermore, the cell proliferation assay and soft agar colony formation assay indicated that knockdown of lnc-MLETA1 significantly decreased the cell growth and anchorage-independent growth of CL1-5 cells compared with the controls (Supplementary Fig. S2C and D). Collectively, these data suggested that lnc-MLETA1 plays a critical role in cell motility and growth.

#### Exosomal lnc-MLETA1 promotes lung cancer cell migration and invasion in vitro

To observe the exosome-mediated transmission of lnc-MLETA1, we biotinylated lnc-MLETA1 and transfected it into CL1-0 cells to collect the exosomes. Subsequently,

the purified exosomes were added to CL1-0 cells. Confocal microscopy analysis showed that CL1-0 cells incubated with exosomes containing biotinylated lnc-MLETA1 had obvious green fluorescent signals, but control cells did not (Fig. 3A). To further determine whether the exosome-mediated transfer of lnc-MLETA1 promotes cell migration and invasion, we first isolated exosomes from lnc-MLETA1-overexpressing CL1-0 cells. qRT-PCR analysis showed that the levels of lnc-MLETA1 were significantly increased in the lnc-MLETA1-overexpressing CL1-0 exosomes compared with the CL1-0 exosomes (Supplementary Fig. S3A). The levels of lnc-MLETA1 in the CL1-0 cells treated with lnc-MLETA1-overexpressing exosomes were significantly higher than those in the cells treated with control exosomes (Supplementary Fig. S3B). Wound-healing assays and transwell invasion assays showed that the lnc-MLETA1-overexpressing exosomes significantly increased the migration and invasion of CL1-0 cells compared with the control exosomes (Fig. 3B and C). These data indicated that exosome-mediated transfer of lnc-MLETA1 could promote cell migration and invasion.

To determine whether the effect of CL1-5 exosomes on cell motility is mediated by the delivery of lnc-MLETA1, we first detected the levels of lnc-MLETA1 in the CL1-0 cells treated with CL1-0 or CL1-5 exosomes. The results showed that lnc-MLETA1 was significantly increased in the CL1-0 cells treated with CL1-5 exosomes compared with those treated with CL1-0 exosomes (Supplementary Fig. S3C). We incubated CL1-0 cells with CL1-5 exosomes and transfected them with lnc-MLETA1 LNA or control LNA. Wound healing assays and transwell invasion assays showed that knockdown of lnc-MLETA1 significantly inhibited CL1-5 exosome-mediated migration and invasion of CL1-0 cells (Fig. 3D and E). Together, these data demonstrated that exosomes derived from CL1-5 cells promote the migration and invasion of CL1-0 cells by delivering lnc-MLETA1.

(See figure on next page.)

**Fig. 4** Exosomal lnc-MLETA1 promotes lung cancer metastasis in vivo. **A** The right lungs of NOD-SCID mice were orthotopically xenografted with lnc-MLETA1-knockdown ( $n=9$ ) or control CL1-5 cells ( $n=7$ ), and the metastases in the left lungs were observed. **B** Representative bioluminescent images and **C** quantification of bioluminescent imaging signal intensities each week for 4 weeks. **D** Representative bioluminescent images (left) and quantification of bioluminescent imaging signal intensities (right) of the left lung of mice were evaluated by the IVIS system ex vivo. **E** Representative images (left) and the number of metastatic tumors (right) in the left lungs of mice were counted. Deep blue arrow heads indicate primary tumors. Red arrow heads indicate lung metastatic tumors. **F** Representative microscopic images of H&E staining (left) and the diameter of the largest metastatic tumor (right) in the left lungs of mice were counted. Red arrow heads indicate lung metastatic tumors. Scale bar, 100  $\mu\text{m}$ . **G** NOD-SCID mice were subcutaneously xenografted with CL1-0 cells and injected intratumorally with exosomes derived from lnc-MLETA1-overexpressing or control CL1-0 cells twice a week ( $n=3$  mice per group). **H** Representative bioluminescent images (left) and quantification of bioluminescent imaging signal intensities (right) of the lung of mice were evaluated by the IVIS system ex vivo. **I** Representative images (left) and the number of metastatic tumors (right) in the lungs of mice were counted. Red arrow heads indicate lung metastatic tumors. **J** Representative microscopic images of H&E staining (left) and the diameter of the largest metastatic tumor (right) in the lungs of mice were counted. Red arrow heads indicate lung metastatic tumors. Scale bar, 100  $\mu\text{m}$ . Results are presented as mean  $\pm$  SD. \* $P < 0.05$ , \*\* $P < 0.01$ . Two-tailed Student's *t*-test

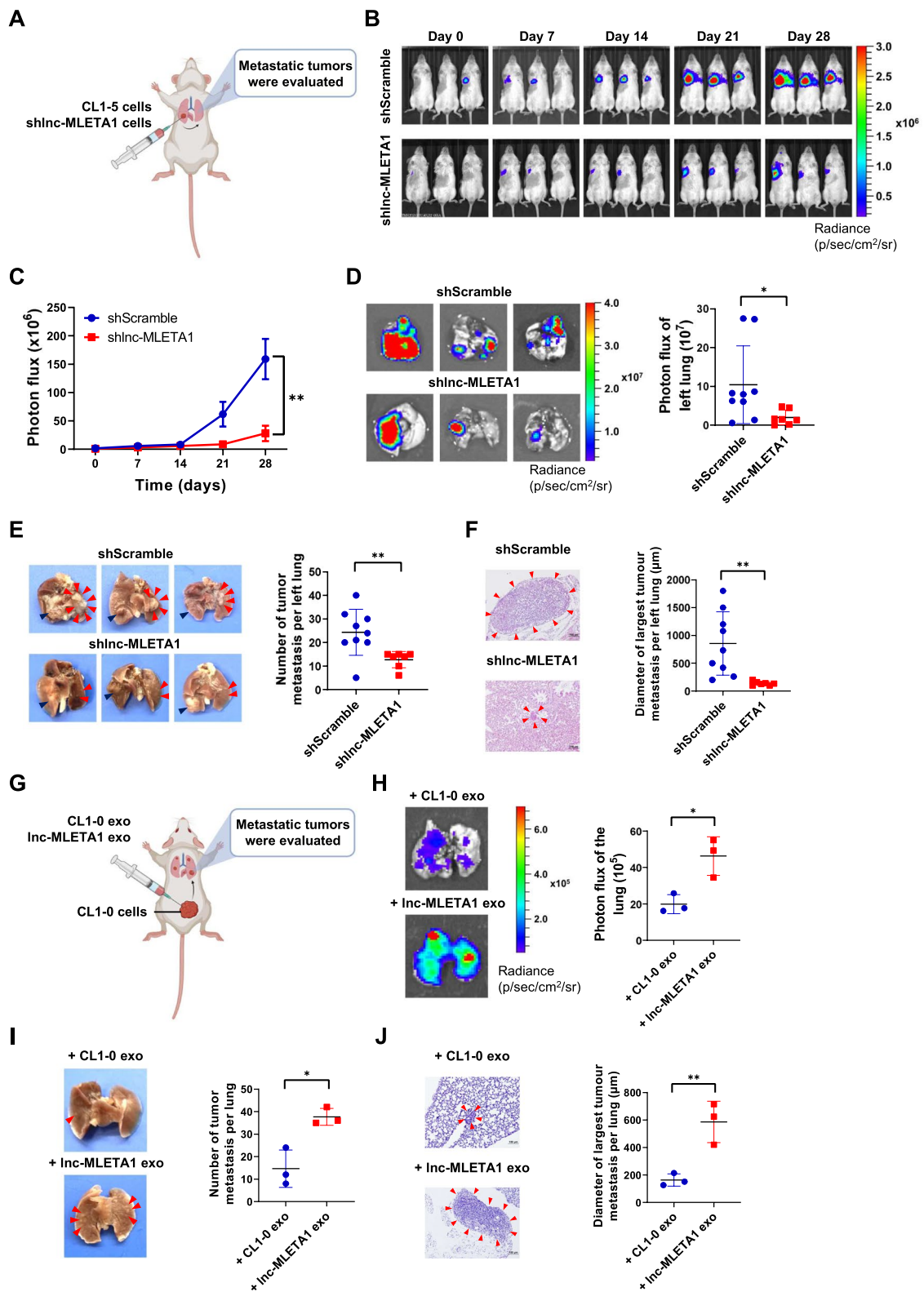


**Fig. 4** (See legend on previous page.)

### Exosomal lnc-MLETA1 promotes lung cancer metastasis in vivo

To examine the role of lnc-MLETA1 in lung cancer metastasis, we established an orthotopic xenograft model in which luciferase-labeled CL1-5 or lnc-MLETA1-knockdown CL1-5 cells were administered via intrapulmonary injection into the right lungs of 6- to 8-week-old male NOD-SCID mice (Fig. 4A). The IVIS spectrum showed that knockdown of lnc-MLETA1 significantly decreased bioluminescent signals compared with those of the control group (Fig. 4B and C). Moreover, IVIS spectrum ex vivo images showed that knockdown of lnc-MLETA1 significantly reduced the bioluminescent signals in the left lungs compared to the controls (Fig. 4D). Furthermore, knockdown of lnc-MLETA1 significantly decreased the number and size of metastatic lesions in the left lungs (Fig. 4E and F). These data suggested that lnc-MLETA1 is required for lung cancer metastasis.

To further determine whether exosomal lnc-MLETA1 promotes lung cancer metastasis, we subcutaneously xenografted luciferase-labeled CL1-0 cells into NOD-SCID mice and intratumorally injected them with exosomes derived from lnc-MLETA1-overexpressing or control CL1-0 cells twice a week (Fig. 4G). At the primary site, we found that exosomal lnc-MLETA1 augments tumor growth (Supplementary Fig. S4A-E). At the metastatic site, IVIS spectrum ex vivo images showed that exosomal lnc-MLETA1 significantly increased the bioluminescent signals in the lungs compared with the controls (Fig. 4H). Furthermore, exosomal lnc-MLETA1 significantly increased the number and size of lung metastatic lesions (Fig. 4I and J). Collectively, these data suggest that exosomal lnc-MLETA1 promotes lung cancer metastasis.

### lnc-MLETA1 interacts with miR-186-5p and miR-497-5p to promote cell motility

Recently, some studies have shown that lncRNAs can act as miRNA sponges to regulate downstream targets of miRNAs [10]. Therefore, we first determined the distribution of lnc-MLETA1 in CL1-5 cells. Cellular RNA fractionation assays revealed that lnc-MLETA1

is predominantly located in the cytoplasm (Fig. 5A). To investigate whether lnc-MLETA1 can interact with miRNAs, we performed an MS2-tagged RNA affinity purification (MS2-TRAP) assay to verify potential miRNA candidates predicted by LncBase Predicted v.2. The results showed that Ago2 was apparently pulled down by MS2-lnc-MLETA1, indicating that lnc-MLETA1 may interact with miRNA (Fig. 5B). The bioinformatic analysis showed that lnc-MLETA1 contained binding sequences for several miRNAs, including miR-186-5p, miR-497-5p, miR-127-5p and miR-375 (Fig. 5C; Supplementary Fig. S5A). Interestingly, RNA pulldown assays revealed significant increases in miR-186-5p and miR-497-5p in the MS2-lnc-MLETA1 pulldown samples compared to the controls (Fig. 5D and E). These data suggested that lnc-MLETA1 can interact with miR-186-5p and miR-497-5p but not miR-127-5p and miR-375.

To further determine the contribution of lncRNA-miRNA interactions to cell motility, we performed a wound-healing assay of CL1-0 and CL1-5 cells co-transfected with lnc-MLETA1 and miRNA mimics. The results showed that overexpression of lnc-MLETA1 significantly increased the number of migrated CL1-0 cells, but this effect was abolished by overexpression of miR-186-5p and miR-497-5p (Fig. 5F; Supplementary Fig. S5B-D). Conversely, miR-186-5p and miR-497-5p mimics significantly decreased the migrated cell number in CL1-5 cells, but this effect could be rescued by overexpression of lnc-MLETA1 (Fig. 5G; Supplementary Fig. S5E-G). In addition, lncRNAs and miRNAs did not exhibit any influence on the expression of each other (Supplementary Fig. S5H-J). The levels of miR-186-5p and miR-497-5p did not differ between CL1-0 and CL1-5 cells (Supplementary Fig. S5K and L). Taken together, these data suggest that lnc-MLETA1 promotes cell motility by sponging miR-186-5p and miR-497-5p.

### lnc-MLETA1 promotes cell motility through the miR-186-5p/EGFR and miR-497-5p/IGF1R axes

To explore the underlying mechanism of lnc-MLETA1-mediated cell motility, we performed RNA sequencing on lnc-MLETA1-knockdown and control CL1-5 cells.

(See figure on next page.)

**Fig. 5** lnc-MLETA1 interacts with miR-186-5p and miR-497-5p to promote cell motility. **A** Cellular RNA fractionation assay of lnc-MLETA1 in CL1-5 cells. **B** Western blot analysis of Ago2 and MS2-GST expression in lysate and the MS2-TRAP RNA pull-down sample. **C** Schematic of predicted binding sites of miR-186-5p, miR-497-5p, miR-127-5p and miR-375 on lnc-MLETA1. **D** qRT-PCR analysis of lnc-MLETA1 expression in the MS2-TRAP RNA pull-down sample. **E** qRT-PCR analysis of miR-186-5p, miR-497-5p, miR-127-5p and miR-375 expression in the MS2-TRAP RNA pull-down sample. **F** Left: representative images of wound-healing assay of CL1-0 cells co-transfected with lnc-MLETA1 plasmids or control plasmids and with miRNA mimics or negative control (NC). Scale bar, 200  $\mu$ m. Right: the number of migrated cells was counted. **G** Left: representative images of wound-healing assay of CL1-5 cells co-transfected with lnc-MLETA1 plasmids or control plasmids and with miRNA mimics or negative control. Scale bar, 200  $\mu$ m. Right: the number of migrated cells was counted. Results are presented as mean  $\pm$  SD from three independent experiments.

\* $P < 0.05$ , \*\* $P < 0.01$ , \*\*\* $P < 0.001$ . Two-tailed Student's *t*-test

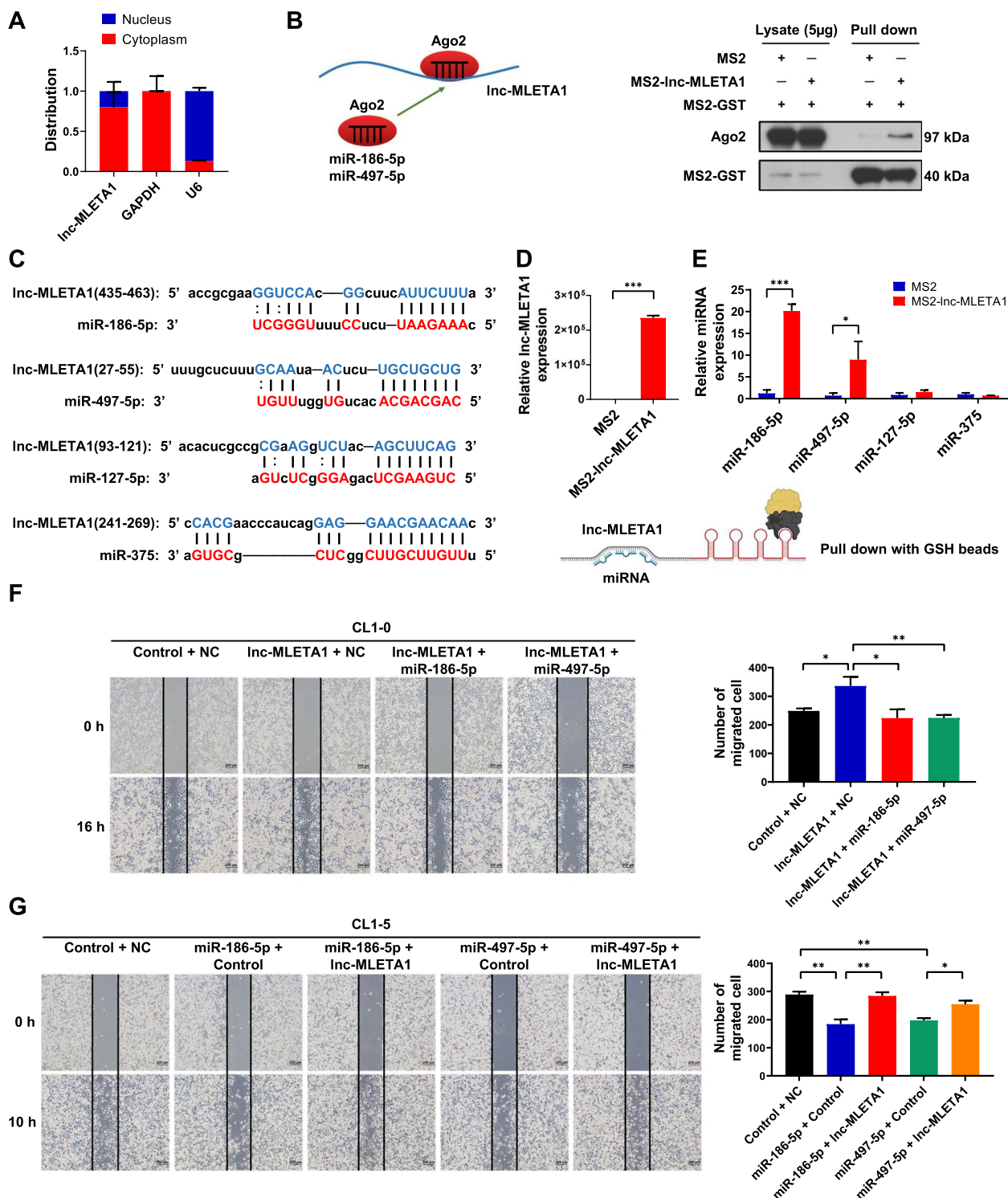


**Fig. 5** (See legend on previous page.)

The heatmap showed the top 50 most increased and decreased genes among 778 differentially-expressed genes (fold change > 2). There are 315 upregulated genes and 463 downregulated genes in lnc-MLETA1-knockdown cells compared with control CL1-5 cells (Fig. 6A). Gene ontology (GO) analysis of the DEGs in lnc-MLETA1-knockdown cells showed 20-term enrichment, such as focal adhesion, integrin complex, and apical plasma membrane (Supplementary Fig. S6A). To further elucidate the effect of lnc-MLETA1 on global metastasis-associated gene changes, we performed gene set enrichment analysis (GSEA) on lnc-MLETA1-knockdown CL1-5 cells. GSEA indicated that three published metastasis-upregulated gene signatures were significantly enriched in downregulated genes (Fig. 6B). Conversely, another three published metastasis-downregulated gene signatures were significantly enriched in upregulated genes, strongly suggesting that lnc-MLETA1 is involved in the metastatic process and regulates the expression of metastasis-related genes. Furthermore, GSEA indicated that target gene signatures of miR-186-5p and miR-497-5p were significantly enriched in downregulated genes (Fig. 6C), suggesting that lnc-MLETA1 modulates the expression of the target genes of miR-186-5p and miR-497-5p that may support metastasis.

Recently, some studies have shown that lncRNAs share miRNAs with mRNAs and thus affect the expression of mRNAs by acting as competing endogenous RNAs [31]. Therefore, we performed a bioinformatic analysis starBase v3.0 to predict the target genes of miR-186-5p and miR-497-5p and to intersect the downregulated genes after silencing lnc-MLETA1 (Fig. 6D). Among these genes, epidermal growth factor receptor (EGFR) and insulin-like growth factor 1 receptor (IGF1R), which have been shown to be associated with lung cancer metastasis and progression [32–35],

were selected for further studies. To verify that EGFR and IGF1R can be regulated by lnc-MLETA1, we performed qRT-PCR analysis and western blot analysis to detect the expression of EGFR and IGF1R after silencing lnc-MLETA1. The results showed that knockdown of lnc-MLETA1 significantly decreased the mRNA and protein expression of EGFR and IGF1R compared with that in the control group (Fig. 6E–H). In addition, GSEA indicated that EGFR and IGF1R signaling-related gene signatures were significantly decreased after lnc-MLETA1 silencing (Supplementary Fig. S6B), suggesting that lnc-MLETA1 regulates the EGFR and IGF1R signaling pathways. To confirm that EGFR and IGF1R can be downregulated by miR-186-5p and miR-497-5p, respectively, we performed qRT-PCR analysis and western blot analysis to detect the expression of EGFR and IGF1R after overexpression of miR-186-5p and miR-497-5p. The results showed that overexpression of miR-186-5p and miR-497-5p significantly decreased the mRNA and protein expression of EGFR and IGF1R compared with that of the control group, respectively (Fig. 6I–L). To further determine whether EGFR and IGF1R are the direct downstream targets of miR-186-5p and miR-497-5p, respectively, we predicted the binding sites of miR-186-5p on the EGFR 3'UTR and miR-497-5p on the IGF1R 3'UTR using starBase v3.0 and performed a luciferase reporter assay of CL1-0 cells transfected with miRNA mimics and pMIR-REPORT luciferase plasmids containing the 3'UTR of EGFR or IGF1R (Supplementary Fig. S6C and D). The results showed that overexpression of miR-186-5p and miR-497-5p significantly decreased the activity of reporter genes containing the 3'UTR of EGFR and IGF1R, respectively (Fig. 6M and N). These data suggested that EGFR and IGF1R are the direct downstream targets of miR-186-5p and miR-497-5p, respectively. To evaluate

(See figure on next page.)

**Fig. 6** lnc-MLETA1 promotes cell motility through the miR-186-5p-EGFR and miR-497-5p-IGF1R axis. **A** RNA-sequencing of total RNA extracted from lnc-MLETA1-knockdown and control CL1-5 cells are presented in a heatmap. **B** Gene Set Enrichment Analysis (GSEA) of published metastasis gene signatures in lnc-MLETA1-knockdown cells versus control cells. **C** GSEA of miRNA target gene signatures in lnc-MLETA1-knockdown cells versus control cells. **D** Left: venn diagram of intersection of predicted miR-186-5p target gene and downregulated gene after silencing lnc-MLETA1. Right: venn diagram of intersection of predicted miR-497-5p target gene and downregulated gene after silencing lnc-MLETA1. **E** qRT-PCR and **F** Western blot analyses of EGFR expression of lnc-MLETA1-knockdown and control CL1-5 cells. **G** qRT-PCR and **H** Western blot analyses of IGF1R expression of lnc-MLETA1-knockdown and control CL1-5 cells. **I** qRT-PCR and **J** Western blot analyses of EGFR expression of miR-186-5p-overexpressing and control CL1-5 cells. **K** qRT-PCR and **L** Western blot analyses of IGF1R expression of miR-497-5p-overexpressing and control CL1-5 cells. **M** Luciferase activity of CL1-0 cells transfected with miR-186-5p mimics and pMIR-REPORT luciferase plasmid which contain 3'UTR of EGFR. Data are presented as the ratio of Renilla luciferase activity to Firefly luciferase activity. **N** Luciferase activity of CL1-0 cells transfected with miR-497-5p mimics and pMIR-REPORT luciferase plasmid which contain 3'UTR of IGF1R. **O** Western blot analysis of EGFR expression of CL1-5 cells co-transfected with lnc-MLETA1 plasmids or control plasmids and with miR-186-5p mimics or negative control. **P** Western blot analysis of IGF1R expression of CL1-5 cells co-transfected with lnc-MLETA1 plasmids or control plasmids and with miR-497-5p mimics or negative control. **Q** Left: representative images of wound-healing assay of CL1-0 cells co-transfected with lnc-MLETA1 plasmids or control plasmids and with shEGFR, shIGF1R, or control shScramble. Scale bar, 200  $\mu$ m. Right: the number of migrated cells was counted. Results are presented as mean  $\pm$  SD from three independent experiments. \* $P$  < 0.05, \*\* $P$  < 0.01, \*\*\* $P$  < 0.001. Two-tailed Student's  $t$ -test

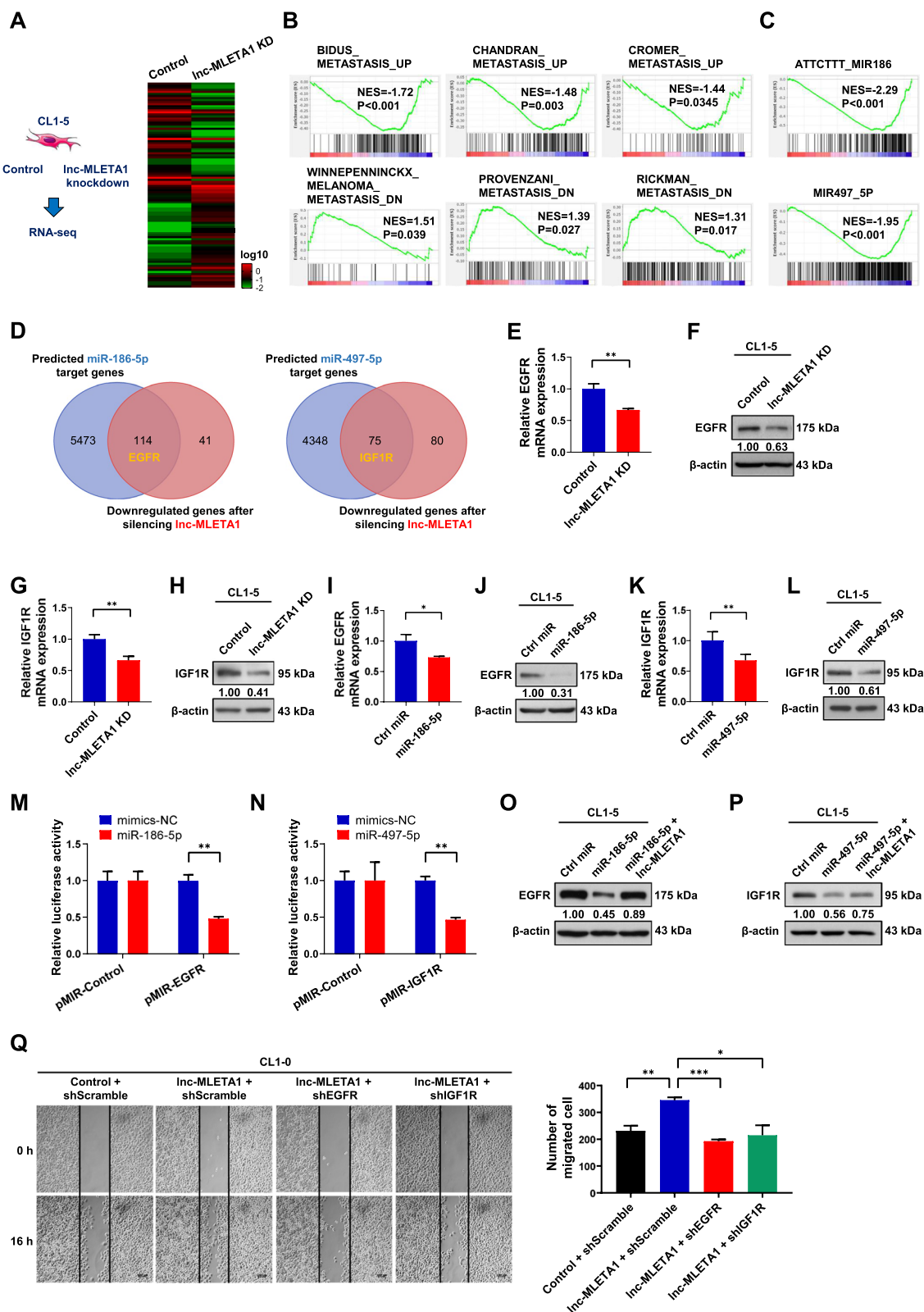


**Fig. 6** (See legend on previous page.)

the contribution of lncRNA–miRNA interactions to the expression of EGFR and IGF1R, we co-transfected CL1-5 cells with lnc-MLETA1 and miRNA mimics. Western blot analysis showed that overexpression of miR-186-5p and miR-497-5p significantly decreased the protein expression of EGFR and IGF1R compared with that of the control group, respectively, but it could be restored by overexpression of lnc-MLETA1 (Fig. 6O and P). To examine the effect of EGFR and IGF1R on lung cancer cell motility, we performed a wound-healing assay on CL1-5 cells infected with EGFR or IGF1R shRNAs. The results showed that knockdown of EGFR and IGF1R significantly decreased the number of migrated CL1-5 cells (Supplementary Fig. S6E–H). To further determine whether lnc-MLETA1 facilitates cell motility via EGFR and IGF1R, we performed a wound-healing assay on CL1-0 cells co-transfected with lnc-MLETA1 and shRNAs targeting EGFR or IGF1R. The results showed that overexpression of lnc-MLETA1 significantly increased the migration of CL1-0 cells, which was abolished by knockdown of EGFR and IGF1R (Fig. 6Q). In aggregate, these data suggested that lnc-MLETA1 promotes cell motility through the miR-186-5p/EGFR and miR-497-5p/IGF1R axes. In addition, to determine whether exosomes derived from CL1-5 cells promote cell migration through EGFR and IGF1R, we performed a wound-healing assay on CL1-0 cells incubated with exosomes derived from CL1-5 cells and transfected with shRNAs targeting EGFR or IGF1R. The results showed that exosomes derived from CL1-5 significantly increased the migration of CL1-0 cells, which was abolished by knockdown of EGFR and IGF1R (Supplementary Fig. S6I). These data suggested that the delivery of exosomes from high-metastatic cancer cells affects low-metastatic cancer migration by upregulating EGFR and IGF1R.

#### Exosomal lnc-MLETA1 was correlated with tumor metastasis in lung cancer patients

We further examined the correlation of lnc-MLETA1 expression and the clinical outcome of lung cancer patients and found that the expression of lnc-MLETA1

was significantly higher in lung cancer tissues than in normal tissues in the Gene Expression Omnibus (GEO) dataset (Fig. 7A). The expression of EGFR and IGF1R was also significantly higher in lung cancer tissues than in normal tissues (Fig. 7B and C). Moreover, lnc-MLETA1 expression was positively correlated with EGFR and IGF1R expression in lung cancer tissues (Fig. 7D and E). Kaplan–Meier analysis revealed that patients with high expression of lnc-MLETA1, EGFR and IGF1R had significantly poorer survival than patients with low expression (Fig. 7F–H). Furthermore, lung cancer patients with both elevated lnc-MLETA1 and EGFR or IGF1R displayed the worst survival, indicating the superior prognostic value of combining the two parameters compared with one gene alone (Fig. 7I and J). In addition, we examined the correlation between the expression of miR-186-5p and miR-497-5p and the clinical outcome of lung cancer patients. The results showed that the expression of miR-186-5p and miR-497-5p was significantly lower in lung cancer tissues than in normal tissues (Supplementary Fig. S7A and B). Moreover, miR-186-5p and miR-497-5p expression was negatively correlated with expression of the target genes EGFR and IGF1R in lung cancer tissues, respectively (Supplementary Fig. S7C and D). Kaplan–Meier analysis indicated that patients with high expression of miR-186-5p and miR-497-5p had significantly better survival than patients with low expression (Supplementary Fig. S7E and F).

Notably, we detected exosomal lnc-MLETA1 levels isolated from plasma samples of lung cancer patients using qRT–PCR analysis and found that elevated expression of exosomal lnc-MLETA1 was significantly associated with higher TNM stage and metastasis in lung cancer patients (Table 1). In addition, the levels of exosomal lnc-MLETA1 in the plasma of lung cancer patients were significantly higher than those in the plasma of healthy subjects (Supplementary Table S1). Receiver operating characteristic (ROC) analysis showed that plasma exosomal lnc-MLETA1 could be a diagnostic biomarker for lung cancer metastasis and discriminated lung cancer patients from healthy subjects (Fig. 7K and L). Intriguingly, we detected the expression of lnc-MLETA1 in the primary and metastatic tissues of lung cancer patients using

(See figure on next page.)

**Fig. 7** lnc-MLETA1 is upregulated in tumor tissues and predicts poor survival in lung cancer patients. **A–C** The expression of lnc-MLETA1 (**A**), EGFR (**B**) and IGF1R (**C**) between non-tumor and tumor tissue in the GSE19188 dataset. The data were analyzed with two-tailed Student's *t*-test. **D** and **E** The Pearson correlation analysis of the expression of lnc-MLETA1 and EGFR (**D**) or IGF1R (**E**) in the GSE19188 dataset. **F–H** Kaplan–Meier analysis of overall survival in lung adenocarcinoma patients with high or low lnc-MLETA1 (**F**), EGFR (**G**) and IGF1R (**H**) expression. **I** and **J** Kaplan–Meier analysis of overall survival in lung adenocarcinoma patients with high- or low-scoring groups using the gene expression of lnc-MLETA1 plus EGFR (**I**) and lnc-MLETA1 plus IGF1R (**J**). The patients were divided into high and low groups based on the median expression value of the gene in the cohort and the data were analyzed with log-rank test. **K** and **L** ROC curve analysis of plasma exosomal lnc-MLETA1 for lung cancer metastasis (**K**) and lung cancer (**L**). Results are presented as mean ± SD. \*\**P* < 0.01, \*\*\**P* < 0.001



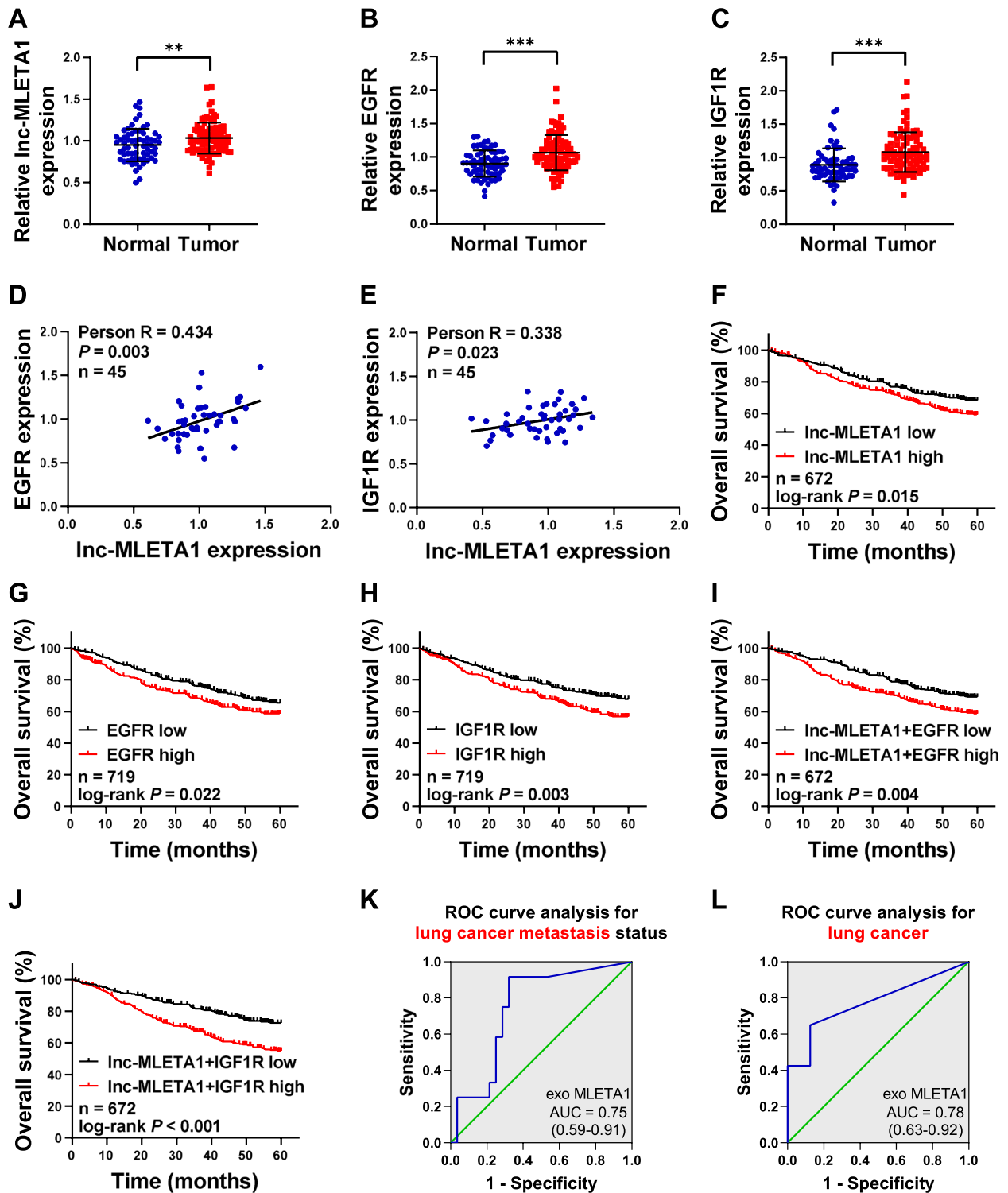


**Fig. 7** (See legend on previous page.)

in situ hybridization staining and found that the levels of Inc-MLETA1 in metastatic tissues were obviously higher than those in primary tissues (Supplementary Fig. S7G).

In conclusion, Inc-MLETA1 is upregulated in highly metastatic cancer cells and their secreted exosomes and predicts the survival of lung cancer patients. Mechanistically,

**Table 1** Correlations between exosomal lnc-MLETA1 expression and clinicopathological features

Variables	Low exo MLETA1 (n=20)	High exo MLETA1 (n=20)	P value
<b>Gender</b>			0.749
Male	9	8	
Female	11	12	
<b>Age</b>			0.705
<60	5	4	
≥60	15	16	
<b>Tumor size (cm)</b>			0.204
<3	11	7	
≥3	9	13	
<b>Recurrence</b>			0.519
No	7	9	
Yes	13	11	
<b>TNM stage</b>			0.011*
I/II	13	5	
III/IV	7	15	
<b>Metastasis</b>			<0.001*
No	19	9	
Yes	1	11	

The expression level of exosomal lnc-MLETA1 was examined by RT-qPCR. The patients were split by the median concentration of lnc-MLETA1 and the data were analyzed with Chi-squared test. P values < 0.05 were considered statistically significant

lnc-MLETA1 promotes cell motility and regulates the expression of EGFR and IGF1R by sponging miR-186-5p and miR-497-5p. Our findings suggest that lnc-MLETA1 plays a critical role in lung cancer metastasis and may serve as a biomarker for lung cancer diagnosis and prognosis and a potential target for lung cancer treatment (Fig. 8).

## Discussion

In recent years, growing evidence has shown that tumor-derived exosomes promote lung cancer metastasis [6, 36]. Although researchers have revealed that exosomal miRNAs or proteins can facilitate lung cancer cell motility and tumor metastasis, the effect of exosomal lncRNAs on lung cancer metastasis remains poorly understood. In the present study, we first identified a novel lncRNA, MLETA1, that was elevated in highly metastatic lung cancer cells and their secreted exosomes. Moreover, lnc-MLETA1 was required for lung cancer cell motility and metastasis. Importantly, lnc-MLETA1 could be packaged into exosomes and disseminated to poorly metastatic cells, leading to lung cancer metastasis. Furthermore, lnc-MLETA1 modulated the expression of EGFR and IGF1R by competitively binding miR-186-5p and miR-497-5p. In addition, we verified that lnc-MLETA1 was upregulated in tumor tissues and correlated with poor survival in lung

cancer patients. Interestingly, exosomal lnc-MLETA1 detected in plasma from lung cancer patients was associated with lung cancer metastasis. Our findings indicate that exosomal lnc-MLETA1 may be a prognostic indicator for metastatic lung cancer and may serve as a therapeutic target for lung cancer treatment.

Extensive evidence indicates that the nuclear or cytoplasmic localization of lncRNAs is associated with the cellular functions of lncRNAs [17]. lncRNAs can interact with miRNAs, mRNAs, and proteins to regulate post-transcriptional modification in the cytoplasm [37, 38]. However, lncRNAs recruit transcription factors and bind promoter regions to modulate gene transcription in the nucleus [39]. Hence, we performed subcellular fractionation to demonstrate that lnc-MLETA1 in lung cancer cells is mainly located in the cytoplasm. lnc-MLETA1 acts as a competitive endogenous RNA to sponge miRNAs and influences the expression of downstream targets of miRNAs. Precursor miRNAs are processed to mature miRNA by Drosha and Dicer and retained in the RNA-induced silencing complex (RISC), which contains the key protein Argonaute 2 (Ago2) [40]. Therefore, an MS2-tagged RNA affinity purification (MS2-TRAP) assay was used to confirm the presence of Ago2 in the MS2-lnc-MLETA1 pulldown samples and demonstrate that lnc-MLETA1 might interact with miRNAs. In parallel, we further verified that lnc-MLETA1 interacts with miR-186-5p and miR-497-5p. Apart from miRNAs, whether lnc-MLETA1 also binds to mRNAs or proteins to promote lung cancer metastasis and progression requires further study. In the future, we will explore the other regulatory mechanisms of lnc-MLETA1 in lung cancer.

Previous studies indicated that EGFR and IGF1R are essential in lung cancer progression [34, 41–43]. Overexpression of EGFR and IGF1R induces lung cancer cell proliferation, migration, invasion, drug resistance, stemness and tumor metastasis. The clinical data revealed that the expression of EGFR and IGF1R is associated with poor outcomes in lung cancer patients. Interestingly, our findings showed that miR-186-5p and miR-497-5p modulate the expression of EGFR and IGF1R by directly binding their 3'UTRs, respectively. Recently, some studies have shown that miR-186-5p and miR-497-5p inhibit lung cancer cell growth, migration, and invasion [44, 45]. Moreover, the expression of miR-186-5p and miR-497-5p was negatively correlated with TNM stage, lymph node metastasis and survival in lung cancer patients, suggesting that miR-186-5p and miR-497-5p are tumor suppressor miRNAs in lung cancer. Importantly, we found that lnc-MLETA1 regulated the expression of EGFR and IGF1R by sponging miR-186-5p and miR-497-5p to facilitate cell motility. Thus, these data indicated that lnc-MLETA1 plays a crucial role in lung cancer progression and metastasis.

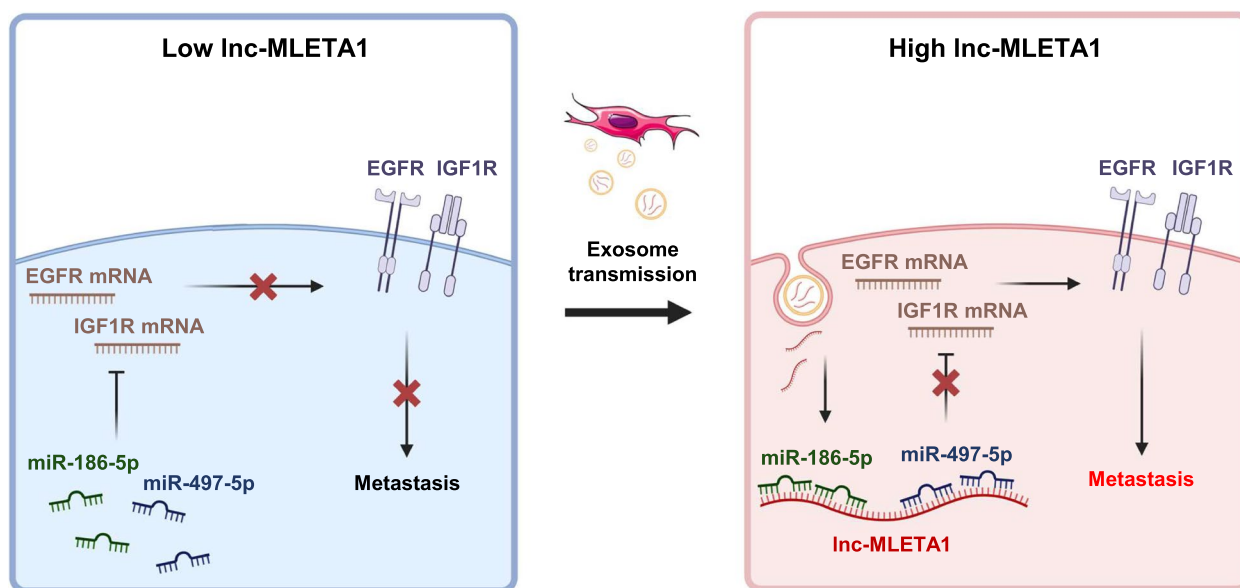


**Fig. 8** Schematic diagram of lnc-MLETA1-based regulatory mechanism in lung cancer metastasis. Exosomal lnc-MLETA1 can be delivered from high metastatic lung cancer cells to low metastatic lung cancer cells. Moreover, lnc-MLETA1 regulates the expression of EGFR and IGF1R by sponging miR-186-5p and miR-497-5p, leading to lung cancer cell motility and metastasis

Antisense oligonucleotide (ASO)-based therapeutics are a promising novel strategy against various diseases, including hypercholesterolemia, Huntington's disease, Alzheimer's disease, Parkinson's disease, Duchenne muscular dystrophy, and cancer [46–48]. ASO drugs are single-stranded chains of synthetic oligonucleotides that specifically bind a target RNA and block its function through Watson–Crick base pairing [49]. As of 2022, the U.S. Food and Drug Administration (FDA) already approved 10 ASO drugs [50]. Although these 10 ASO drugs are not for cancer, other anticancer ASO candidates have entered clinical development [51]. Moreover, researchers are still investigating the underlying mechanisms of lncRNA-mediated tumor progression and attempting to design specific locked nucleic acid antisense oligonucleotides (LNA ASOs) to target lncRNAs. For example, Qu et al. found that targeting lncARSR with LNA ASO-based treatment overcame drug resistance in advanced renal cell carcinoma [31]. Tan et al. found that targeting EGFR-AS1 with LNA induced tumor regression in squamous cell carcinoma [52]. In our study, we designed an LNA against lnc-MLETA1 and found that specific targeting of lnc-MLETA1 suppressed highly metastatic lung cancer cell-derived exosome-mediated cell migration and invasion. In the future, we will further examine the effect of LNA or other strategies targeting lnc-MLETA1 on lung cancer metastasis in vivo, hoping that lncRNA-targeted therapy could be applied as a novel therapeutic strategy for lung cancer treatment.

## Conclusions

This study identifies lnc-MLETA1 as a critical exosomal lncRNA that mediates crosstalk in lung cancer cells to promote cancer metastasis and may serve as a prognostic biomarker and potential therapeutic target for lung cancer diagnosis and treatment.

## Abbreviations

lncRNA	Long noncoding RNA
NSCLC	Non-small cell lung cancer
RNA-seq	RNA sequencing
qRT-PCR	Quantitative real-time polymerase chain reaction
MS2-TRAP	MS2-tagged RNA affinity purification assay
ceRNA	Competing endogenous RNA
EGFR	Epidermal growth factor receptor
IGF1R	Insulin like growth factor 1 receptor

## Supplementary Information

The online version contains supplementary material available at <https://doi.org/10.1186/s13046-023-02859-y>.

**Additional file 1: Supplementary Figure 1.** Characterization of lnc-MLETA1. **Supplementary Figure 2.** Knockdown of lnc-MLETA1 suppresses cell growth and anchorage-independent growth ability of lung cancer cell. **Supplementary Figure 3.** Exosome-transmitted lnc-MLETA1 is uptake by CL1-0 cells. **Supplementary Figure 4.** Exosomal lnc-MLETA1 augments tumor growth in vivo. **Supplementary Figure 5.** Regulatory relationships between lnc-MLETA1 and miR-186-5p or miR-497-5p. **Supplementary Figure 6.** Knockdown of EGFR and IGF1R attenuates lung cancer cell migration. **Supplementary Figure 7.** miR-186-5p and miR-497-5p are downregulated in tumor tissues and predicts good survival in lung cancer patients. **Supplementary Table S1.** Correlations between exosomal lnc-MLETA1 expression and lung cancer diagnosis. **Supplementary Table S2.** Sequences of primers/shRNA/LNA used in this study.

### Acknowledgements

We are grateful for the supports from the Laboratory Animal Center, College of Medicine, National Cheng Kung University and Taiwan Animal Consortium. We thank the technical services provided by the "RNAi Core" and the "Immunobiology Core", Clinical Medicine Research Center, National Cheng Kung University Hospital, Taiwan. We thank the National RNAi Core Facility at Academia Sinica in Taiwan for providing shRNA reagents and related services.

### Authors' contributions

Conceptualization, TM Hong; methodology, XR Hsu, JE Wu, and YY Wu; investigation, XR Hsu, JE Wu, and YY Wu; resources, YL Chen and TM Hong; data curation and writing-original draft preparation, XR Hsu; writing-review and editing, YL Chen; supervision, TM Hong; project administration, TM Hong; funding acquisition, YL Chen and TM Hong; clinical sample collection, SY Hsiao, JL Liang, and YJ Wu; statistical analyses, CH Tung and MF Huang; experimental techniques and material support, MS Lin and PC Yang. All authors have read and agreed to the published version of the manuscript.

### Funding

This study was supported by grants from the Ministry of Science and Technology, Taiwan (MOST 107-2314-B-006-068-MY3, MOST 109-2314-B-006-057-MY3, MOST 110-2314-B-006-073-MY3, MOST 110-2314-B-006-097-MY3, MOST 111-2311-B-006-004-MY3), and Chi Mei Medical Center, Liouying (CLFHR10933).

### Availability of data and materials

All data generated or analyzed during this study are included in this published article and its supplementary information files.

### Declarations

#### Ethics approval and consent to participate

The study was conducted in accordance with the Declaration of Helsinki and approved by the Institutional Review Board of Chi Mei Hospital (11006-L02), and all patients signed an informed consent. The animal study protocol was approved by the Institutional Animal Care and Use Committee of National Cheng Kung University (IACUC Approval No. 107119, Tainan, Taiwan).

#### Consent for publication

All authors agreed with submission of the manuscript for publication and agree to be accountable for all aspect of the manuscript.

#### Competing interests

The authors declare that they have no competing interests.

#### Author details

<sup>1</sup>Institute of Clinical Medicine, College of Medicine, National Cheng Kung University, Tainan, Taiwan. <sup>2</sup>Clinical Medicine Research Center, National Cheng Kung University Hospital, College of Medicine, National Cheng Kung University, Tainan, Taiwan. <sup>3</sup>Department of Internal Medicine, Division of Hematology-Oncology, Chi Mei Medical Center, Liouying, Tainan, Taiwan. <sup>4</sup>Department of Surgery, Chi-Mei Medical Center, Liouying, Tainan, Taiwan. <sup>5</sup>Department of Pathology, Chi Mei Medical Center, Liouying, Tainan, Taiwan. <sup>6</sup>Institute of Biomedical Sciences, Academia Sinica, Taipei 115, Taiwan. <sup>7</sup>Department of Internal Medicine, College of Medicine, National Taiwan University, Taipei 100, Taiwan. <sup>8</sup>YongLin Institute of Health, National Taiwan University, Taipei, Taiwan. <sup>9</sup>Institute of Oral Medicine, College of Medicine, National Cheng Kung University, Tainan, Taiwan.

Received: 2 June 2023 Accepted: 10 October 2023

Published online: 26 October 2023

### References

- Siegel RL, Miller KD, Wagle NS, Jemal A. Cancer statistics, 2023. *CA Cancer J Clin*. 2023;73(1):17–48.
- Herbst RS, Morgensztern D, Boshoff C. The biology and management of non-small cell lung cancer. *Nature*. 2018;553(7689):446–54.
- Torre LA, Siegel RL, Jemal A. Lung cancer statistics. *Adv Exp Med Biol*. 2016;893:1–19.
- Ali A, Goffin JR, Arnold A, Ellis PM. Survival of patients with non-small-cell lung cancer after a diagnosis of brain metastases. *Curr Oncol*. 2013;20(4):e300–6.
- Chen C, Luo Y, He W, Zhao Y, Kong Y, Liu H, et al. Exosomal long noncoding RNA LNMAT2 promotes lymphatic metastasis in bladder cancer. *J Clin Invest*. 2020;130(1):404–21.
- Jiang C, Zhang N, Hu X, Wang H. Tumor-associated exosomes promote lung cancer metastasis through multiple mechanisms. *Mol Cancer*. 2021;20(1):117.
- Shang A, Gu C, Wang W, Wang X, Sun J, Zeng B, et al. Exosomal circ-PACRGL promotes progression of colorectal cancer via the miR-142-3p/miR-506-3p-TGF- $\beta$ 1 axis. *Mol Cancer*. 2020;19(1):117.
- Wang L, Wang J, Yin X, Guan X, Li Y, Xin C, et al. GIPC2 interacts with Fzd7 to promote prostate cancer metastasis by activating WNT signaling. *Oncogene*. 2022;41(18):2609–23.
- Qiu S, Xie L, Lu C, Gu C, Xia Y, Lv J, et al. Gastric cancer-derived exosomal miR-519a-3p promotes liver metastasis by inducing intrahepatic M2-like macrophage-mediated angiogenesis. *J Exp Clin Cancer Res*. 2022;41(1):296.
- Schmitt AM, Chang HY. Long Noncoding RNAs in Cancer Pathways. *Cancer Cell*. 2016;29(4):452–63.
- Statello L, Guo CJ, Chen LL, Huarte M. Gene regulation by long non-coding RNAs and its biological functions. *Nat Rev Mol Cell Biol*. 2021;22(2):96–118.
- Xue ST, Zheng B, Cao SQ, Ding JC, Hu GS, Liu W, et al. Long non-coding RNA LINC00680 functions as a ceRNA to promote esophageal squamous cell carcinoma progression through the miR-423-5p/PAK6 axis. *Mol Cancer*. 2022;21(1):69.
- Wang X, Cheng H, Zhao J, Li J, Chen Y, Cui K, et al. Long noncoding RNA DLGAP1-AS2 promotes tumorigenesis and metastasis by regulating the Trim21/ELOA/LHPP axis in colorectal cancer. *Mol Cancer*. 2022;21(1):210.
- Zhou Y, Shao Y, Hu W, Zhang J, Shi Y, Kong X, et al. A novel long noncoding RNA SP100-AS1 induces radioresistance of colorectal cancer via sponging miR-622 and stabilizing ATG3. *Cell Death Differ*. 2023;30(1):11–24.
- Zhou M, Pan S, Qin T, Zhao C, Yin T, Gao Y, et al. LncRNA FAM83H-AS1 promotes the malignant progression of pancreatic ductal adenocarcinoma by stabilizing FAM83H mRNA to protect  $\beta$ -catenin from degradation. *J Exp Clin Cancer Res*. 2022;41(1):288.
- Zhu Q, Zhang C, Qu T, Lu X, He X, Li W, et al. MNX1-AS1 Promotes Phase Separation of IGF2BP1 to Drive c-Myc-Mediated Cell-Cycle Progression and Proliferation in Lung Cancer. *Cancer Res*. 2022;82(23):4340–58.
- Bridges MC, Daulagala AC, Kourtidis A. LNCcation: lncRNA localization and function. *J Cell Biol*. 2021;220(2):e202009045.
- Liu SJ, Dang HX, Lim DA, Feng FY, Maher CA. Long noncoding RNAs in cancer metastasis. *Nat Rev Cancer*. 2021;21(7):446–60.
- Li D, She J, Hu X, Zhang M, Sun R, Qin S. The ELF3-regulated lncRNA UBE2CP3 is over-stabilized by RNA-RNA interactions and drives gastric cancer metastasis via miR-138-5p/ITGA2 axis. *Oncogene*. 2021;40(35):5403–15.
- Wu N, Jiang M, Liu H, Chu Y, Wang D, Cao J, et al. LINC00941 promotes CRC metastasis through preventing SMAD4 protein degradation and activating the TGF- $\beta$ /SMAD2/3 signaling pathway. *Cell Death Differ*. 2021;28(1):219–32.
- Wen S, Wei Y, Zen C, Xiong W, Niu Y, Zhao Y. Long non-coding RNA NEAT1 promotes bone metastasis of prostate cancer through N6-methyladenosine. *Mol Cancer*. 2020;19(1):171.
- Fan T, Sun N, He J. Exosome-derived lncRNAs in lung cancer. *Front Oncol*. 2020;10:1728.
- Zang X, Gu J, Zhang J, Shi H, Hou S, Xu X, et al. Exosome-transmitted lncRNA UFC1 promotes non-small-cell lung cancer progression by EZH2-mediated epigenetic silencing of PTEN expression. *Cell Death Dis*. 2020;11(4):215.
- Zhang R, Xia Y, Wang Z, Zheng J, Chen Y, Li X, et al. Serum long non-coding RNA MALAT-1 protected by exosomes is up-regulated and promotes cell proliferation and migration in non-small cell lung cancer. *Biochem Biophys Res Commun*. 2017;490(2):406–14.
- Lei Y, Guo W, Chen B, Chen L, Gong J, Li W. Tumor-released lncRNA H19 promotes gefitinib resistance via packaging into exosomes in non-small cell lung cancer. *Oncol Rep*. 2018;40(6):3438–46.

26. Wang PS, Chou CH, Lin CH, Yao YC, Cheng HC, Li HY, et al. A novel long non-coding RNA linc-ZNF469-3 promotes lung metastasis through miR-574-5p-ZEB1 axis in triple negative breast cancer. *Oncogene*. 2018;37(34):4662–78.
27. Rodrigues G, Hoshino A, Kenific CM, Matei IR, Steiner L, Freitas D, et al. Tumour exosomal CEMIP protein promotes cancer cell colonization in brain metastasis. *Nat Cell Biol*. 2019;21(11):1403–12.
28. Yang B, Feng X, Liu H, Tong R, Wu J, Li C, et al. High-metastatic cancer cells derived exosomal miR92a-3p promotes epithelial-mesenchymal transition and metastasis of low-metastatic cancer cells by regulating PTEN/Akt pathway in hepatocellular carcinoma. *Oncogene*. 2020;39(42):6529–43.
29. Wu K, Feng J, Lyu F, Xing F, Sharma S, Liu Y, et al. Exosomal miR-19a and IBSP cooperate to induce osteolytic bone metastasis of estrogen receptor-positive breast cancer. *Nat Commun*. 2021;12(1):5196.
30. Qi M, Xia Y, Wu Y, Zhang Z, Wang X, Lu L, et al. Lin28B-high breast cancer cells promote immune suppression in the lung pre-metastatic niche via exosomes and support cancer progression. *Nat Commun*. 2022;13(1):897.
31. Qu L, Ding J, Chen C, Wu ZJ, Liu B, Gao Y, et al. Exosome-transmitted lincARSR Promotes Sunitinib resistance in renal cancer by acting as a competing endogenous RNA. *Cancer Cell*. 2016;29(5):653–68.
32. Zhu J, Cai T, Zhou J, Du W, Zeng Y, Liu T, et al. CD151 drives cancer progression depending on integrin  $\alpha 3 \beta 1$  through EGFR signaling in non-small cell lung cancer. *J Exp Clin Cancer Res*. 2021;40(1):192.
33. Sun Y, Gao Y, Dong M, Li J, Li X, He N, et al. Kremen2 drives the progression of non-small cell lung cancer by preventing SOCS3-mediated degradation of EGFR. *J Exp Clin Cancer Res*. 2023;42(1):140.
34. Alfaro-Arnedo E, López IP, Piñero-Hermida S, Canalejo M, Gotera C, Sola JJ, et al. IGF1R acts as a cancer-promoting factor in the tumor microenvironment facilitating lung metastasis implantation and progression. *Oncogene*. 2022;41(28):3625–39.
35. Hua J, Wang X, Ma L, Li J, Cao G, Zhang S, et al. CircVAPA promotes small cell lung cancer progression by modulating the miR-377-3p and miR-494-3p/IGF1R/AKT axis. *Mol Cancer*. 2022;21(1):123.
36. Yin L, Liu X, Shao X, Feng T, Xu J, Wang Q, et al. The role of exosomes in lung cancer metastasis and clinical applications: an updated review. *J Transl Med*. 2021;19(1):312.
37. Huang WJ, Guo SB, Shi H, Li XL, Zhu Y, Li M, et al. The  $\beta$ -catenin-LINC00183-miR-371b-5p-Smad2/LEF1 axis promotes adult T-cell lymphoblastic lymphoma progression and chemoresistance. *J Exp Clin Cancer Res*. 2023;42(1):105.
38. Zhang N, Wang B, Ma C, Zeng J, Wang T, Han L, et al. LINC00240 in the 6p22.1 risk locus promotes gastric cancer progression through USP10-mediated DDX21 stabilization. *J Exp Clin Cancer Res*. 2023;42(1):89.
39. Huang W, Li H, Yu Q, Xiao W, Wang DO. LncRNA-mediated DNA methylation: an emerging mechanism in cancer and beyond. *J Exp Clin Cancer Res*. 2022;41(1):100.
40. Donker RB, Mouillet JF, Nelson DM, Sadovsky Y. The expression of Argonaute2 and related microRNA biogenesis proteins in normal and hypoxic trophoblasts. *Mol Hum Reprod*. 2007;13(4):273–9.
41. Wu S, Luo M, To KKW, Zhang J, Su C, Zhang H, et al. Intercellular transfer of exosomal wild type EGFR triggers osimertinib resistance in non-small cell lung cancer. *Mol Cancer*. 2021;20(1):17.
42. Yang H, Wen L, Zhao C, Li X, Shan C, Liu D, et al. EGFR amplification is a putative resistance mechanism for NSCLC-LM patients with TKI therapy and is associated with poor outcome. *Front Oncol*. 2022;12:902664.
43. Al-Saad S, Richardsen E, Kilvaer TK, Donnem T, Andersen S, Khanekkenari M, et al. The impact of MET, IGF-1, IGF1R expression and EGFR mutations on survival of patients with non-small-cell lung cancer. *PLoS One*. 2017;12(7):e0181527.
44. Wang J, Zhang Y, Ge F. MiR-186 Suppressed Growth, Migration, and Invasion of Lung Adenocarcinoma Cells via Targeting Dicer1. *J Oncol*. 2021;2021:6217469.
45. Huang X, Wang L, Liu W, Li F. MicroRNA-497-5p inhibits proliferation and invasion of non-small cell lung cancer by regulating FGF2. *Oncol Lett*. 2019;17(3):3425–31.
46. Herkt M, Thum T. Pharmacokinetics and proceedings in clinical application of nucleic acid therapeutics. *Mol Ther*. 2021;29(2):521–39.
47. Shadid M, Badawi M, Abulrob A. Antisense oligonucleotides: absorption, distribution, metabolism, and excretion. *Expert Opin Drug Metab Toxicol*. 2021;17(11):1281–92.
48. Bennett CF, Kordasiewicz HB, Cleveland DW. Antisense drugs make sense for neurological diseases. *Annu Rev Pharmacol Toxicol*. 2021;61:831–52.
49. Roberts TC, Langer R, Wood MJA. Advances in oligonucleotide drug delivery. *Nat Rev Drug Discov*. 2020;19(10):673–94.
50. Alhamadani F, Zhang K, Parikh R, Wu H, Rasmussen TP, Bahal R, et al. Adverse drug reactions and toxicity of the food and drug administration-approved antisense oligonucleotide drugs. *Drug Metab Dispos*. 2022;50(6):879–87.
51. Zhou T, Kim Y, MacLeod AR. Targeting long noncoding rna with antisense oligonucleotide technology as cancer therapeutics. *Methods Mol Biol*. 2016;1402:199–213.
52. Tan DSW, Chong FT, Leong HS, Toh SY, Lau DP, Kwang XL, et al. Long non-coding RNA EGFR-AS1 mediates epidermal growth factor receptor addiction and modulates treatment response in squamous cell carcinoma. *Nat Med*. 2017;23(10):1167–75.

## Publisher's Note

Springer Nature remains neutral with regard to jurisdictional claims in published maps and institutional affiliations.

**Ready to submit your research? Choose BMC and benefit from:**

- fast, convenient online submission
- thorough peer review by experienced researchers in your field
- rapid publication on acceptance
- support for research data, including large and complex data types
- gold Open Access which fosters wider collaboration and increased citations
- maximum visibility for your research: over 100M website views per year

**At BMC, research is always in progress.**

Learn more [biomedcentral.com/submissions](https://biomedcentral.com/submissions)

